



Nonreciprocity of Long-range Reverberation in Wedged Continental Shelf

8-25-92

J. X. Zhou, X. Z. Zhang and P. H. Rogers

(School of Mechanical Engineering, Georgia Tech)

D. H. Guan

(Institute of Acoustics, Academia Sinica)

N00014-89-J-1839

DTIC.
ELECTE
SEP 03 1992
S A D

Today we would like to discuss some problems involving Long-range reverberation in shallow water.

Fig. 1

The title of the talk is "Nonreciprocity of Long-range Reverberation in Wedged Continental Shelf". The talk is divided into four parts. First we would like to talk a little bit about the background of current research on long-range reverberation in shallow water. The problem seems to fall into a "dilemma" (endless loop) with no way out. Second, we introduced an averaged angular power spectrum method for long-range reverberation in the Pekeris model to show how we could bypass such 'dilemma'. Based on a resulted transformation relation between arbitrary angle dependence of bottom scattering and the range dependence of reverberation in shallow water, some experimental data on bottom scattering at small grazing angles and low frequencies will be given in the third part. In the last part, using the WKB approximation to the adiabatic normal mode theory, we extend the problem into wedged homogeneous shallow water. The result shows that the monostatic reverberation intensities, obtained at two terminals with different depths, would not be reciprocal. Because of time limitations, the results are presented, rather than developed.

This document has been approved
for public release and sale; its
distribution is unlimited.

407613
92-23932

35 p8

92 8 28 035

I. The status of current research on long-range reverberation in shallow water

Fig.2

Generally speaking, the 'long-range' means low-frequency, and the range is more than several hundred times of water depth. Here are two typical long-range reverberation decay curves for two frequencies(1000Hz, 1600Hz; 1/3 OCT), obtained from a shallow water with the depth of 29m using a explosive source. The ordinate is the relative reverberation level; The abscissa is the range-depth ratio. If a water depth is 100m, the ratio value of 400 corresponds that the reverberation signal comes from 40 km far away.. These reverberation curves(see Fig.1) were obtained in a Pekeris shallow water , i.e., the simplest shallow water model.

Fig.3

In the Pekeris model, the effect grazing angle of sound propagation can be expressed as Eq.(1), where Q is the bottom reflection-loss parameter at small grazing angle, defined as

$$-\ln|V(\theta)| = Q\theta$$

DTIC QUALITY INSPECTED 3

Here are some Zhou's experimental results(from vertical coherence measurements of sound propagation), compared with Zhou and Smith theory. The results show that at long-range, the grazing angles of sound interacting with bottom are very small. For example, at a distance of 400 times of water, the main energy come from angles that are less 2.4° for 800Hz, less than 2° for 1600 Hz. Due to mode stripping, the farther the distance, the smaller the grazing angles of the effective sound propagation. What

Statement A per telecon Marshall ORR
ONR/Code 1125
Arlington, VA 22217-5000
NWW 9/2/92

Dist	Area Code/Spec
A-1	

about the bottom scattering at such small grazing angles and low frequencies?

Fig.4

The upper curves of Fig.4 is a copied from Urick's book. At small grazing angles , no data. The following is quoted from the proceedings of 1983 Shallow Water Acoustics Workshop:

"Grazing angles of primary importance to shallow water applications range from about 30° to near 0° with the smaller angles being more important..... To date, NOVOCEANO has not been able to report either bottom reflectivity or bottom backscattering values for any shallow water area."

Nine years have past, as we know, still no any progress in this area. The multipath in shallow water and the unclear mechanisms of bottom scattering at low frequency make the computation of long-range reverberation very complex. The theoretical acousticians have no adequate and reliable data base for bottom scattering to develop a practical theoretical model. Experimental acousticians say we have no suitable theoretical reverberation formula to use for measuring bottom scattering strength at small grazing angle. (Because the significant difficulty is that if the assumption used in extracting the scattering coefficients from the received reverberation has no enough data as a base, the resulting coefficients will not represent valid environmental parameters which should be independent of how the data were obtained and analyzed.) Thus the problem of long-range reverberation in shallow water seems to fall into an endless loop with no way out.

Some groups are working on developing theoretical model of bottom scattering at low frequency, and trying to get its angular and frequency dependence. A pressing problem is that how to judge the validity of their theoretical results at low frequency

and low grazing angle.(Currently available data are limited to high frequencies or larger grazing angles.)

Next we would like briefly to introduce a averaged angular power spectrum method for shallow water long-range reverberation, and to give some data on bottom scattering at small grazing angles and low frequencies.

II. An averaged angular power spectrum method for long-range reverberation

Fig. 5

For a point source in shallow water, applying the WKB approximation to the normal mode expression(Brekhovskih,Zhou), or using the ray method(Smith) or the flux method(Weston) the averaged sound field intensity can be expressed as Eq.(2)

where $\theta(z_0)$ and $\theta(z)$ are the equivalent ray angle of normal mode at the source depth or receiver depth, S is mode cycle distance. $\ln|V(\theta)|$ is the bottom reflection-loss.

We call I_{ap} the angular power spectrum. Except the cylindrical spreading and the medium absorption, the sound velocity profile and the boundary condition together compose a angular filter of shallow water sound propagation. The angular expression of sound propagation can naturally be connected with the classical expression of bottom scattering in the angular domain. For a given signal duration, there are a lot of scattering signal simultaneously return to a receiver. The bottom scattering looks like a stochastic filter. The reverberation can be treated as a angle-weighted process. The net analog of shallow water reverberation can be expressed as Eq. (3). The forward transmission net, bottom scattering net plus backward transmission net.

Where the $M(\theta, \phi)$ is the bottom scattering coefficient for plane wave. θ is the

grazing angle of incident mode-ray, and ϕ is the scattering angle. A is a scattering area. The validity of a theoretical result from this expression will depend on the validity of scattering coefficient $M(\theta, \phi)$. Unfortunately as above-mentioned, at low frequencies and low grazing angles there is no data or general expression about the $M(\theta, \phi)$. It would be very complex function of bottom surface roughness, sediment type, sediment inhomogeneity, angle, frequency and so on. It still seems no way out.

Here we use a little trick to bypass the "endless loop".

Fig.6

Here is an arbitrary angle dependence of bottom scattering, ignoring the concrete analytical expression, i.e., no matter what is the main mechanism of bottom scattering, surface roughness, volume inhomogeneity or whatever. General speaking, The scattering coefficient $M(\theta, \phi)$ is a slowly changed function. The smaller the angle θ or ϕ , the smaller the scattering strength. If we consider backward scattering is reciprocal, i.e., $M(\theta, \phi) = M(\phi, \theta)$, then at small grazing angles any scattering function can always be expressed as Eqs.(4-5).

We introduce this phenomenological expression only as a "bridge" between long-range reverberation and bottom scattering, ignoring the concrete analytical expression. Next we will see that it is this little trick to help us to bypass the above-mentioned "endless loop".

Fig.7

In the Pekeris model the angular power spectrum is expressed by Eq.(6).

From Eqs.(3-6), we get an expression for long-range reverberation as Eqs.(7-8).

(The reverberation time $t_i = \frac{2r_i}{c}$, c -sound velocity.)

The result shows that the characteristics of long-range reverberation between distance r_{i-1} and r_i mainly depend on the bottom scattering indices μ_i, n_i in the region between θ_{i-1} and θ_i . The transformation between the range dependence of reverberation level RL and the angle dependence of bottom backscattering strength is shown in Fig.7.

From this transformation relation the scattering indices μ_i and n_i can be derived from two data on the experimental curve of reverberation level near r_i . Then we obtain the bottom backscattering strength at the angle θ_i (see Eq.(1)).

III. The reverberation-derived bottom scattering strength at small grazing angels.

Fig. 8

The bottom scattering strength for frequency band of $800Hz-4kHz$ and grazing angles of $2^\circ-8^\circ$, shown here, is derived from at-sea experimental reverberation data.

For the reliability of results only those experimental long-range reverberation data were used for extracting bottom scattering that were about 9 dB higher than the environmental noise. (For comparison, the bottom scattering at larger angles obtained by other researchers from deep water measurements is included with dotted or dashed lines.)

Fig. 9

Here(Fig. 9) is the bottom scattering strength derived from another reverberation

experiment.

Fig. 10

Russian acousticians Ivakin and Lysanov compared their theoretical bottom scattering model with our experimental data (Fig. 10), the discrepancy does not exceed 3 dB at any of the investigated angles and frequencies. Our results have two specific features which are different from high frequency results: **bottom scattering has more strong frequency dependence, and decrease much more rapidly as the grazing angle is decreased.** At very small angles, the bottom scattering index could be larger than Lambert's law scattering i.e., $n > 2$.

IV. Long-range reverberation in wedged homogeneous continental shelf

Fig. 11

Next we extend the results of long-range reverberation to shallow water of variable depth. (we consider the case of propagation directly up or down slop from the source)

If the water depth and sound velocity profile vary extremely slowly with horizontal distance, by neglecting any coupling between normal modes, Pierce obtained a adiabatic normal mode expression for sound propagation as Eq.(9) (a cylindrical coordinate has been assumed):

where

The adiabatic mode theory means that the local modes adapt to local environment. So the grazing angle of equivalent ray of normal modes satisfies Eqs.(10-11).

For a wedged homogeneous continental shelf the water depth can be expressed by

Eq.(12).

Applying WKB approximation to the Pierce's expression, the averaged sound intensity in homogeneous wedged shallow water can be expressed as Eq.(13).

The averaged angular power spectrum in wedged water is expressed by Eq.(14).

Fig. 12

Using above-mentioned angular power spectrum method, we get a averaged sound intensity in the most interested three-half law field area as Eq.(15). The averaged reverberation intensity is expressed by Eq.(16).

The sound propagation is reciprocal if we exchange the positions of the source and receiver. But the monostatic reverberation intensities, obtained at two terminations with a depth of H_1 or H_2 , would not be reciprocal (see Eq.(17)).

Here N is the angular index of bottom scattering defined as Eq.(18). If there are two identical active sonars, but the water depth of their locations is different, the reverberation interference to the sonar at shallower area would be much smaller. For example, if $H_1 = 50m$, $H_2 = 200m$, $N = 2$ (so-call the Lambert's law scattering), then the reverberation interference at shallower area would be 12 dB less.

At last year's Shallow Water Acoustic Workshop held at Woods Hole, a report from NUSC, New London mentioned that the reverberation in continental shelf is not reciprocal. The authors of this talk hope their theoretical result could be, in some degree, helpful to explain the NUSC at-sea experiments.

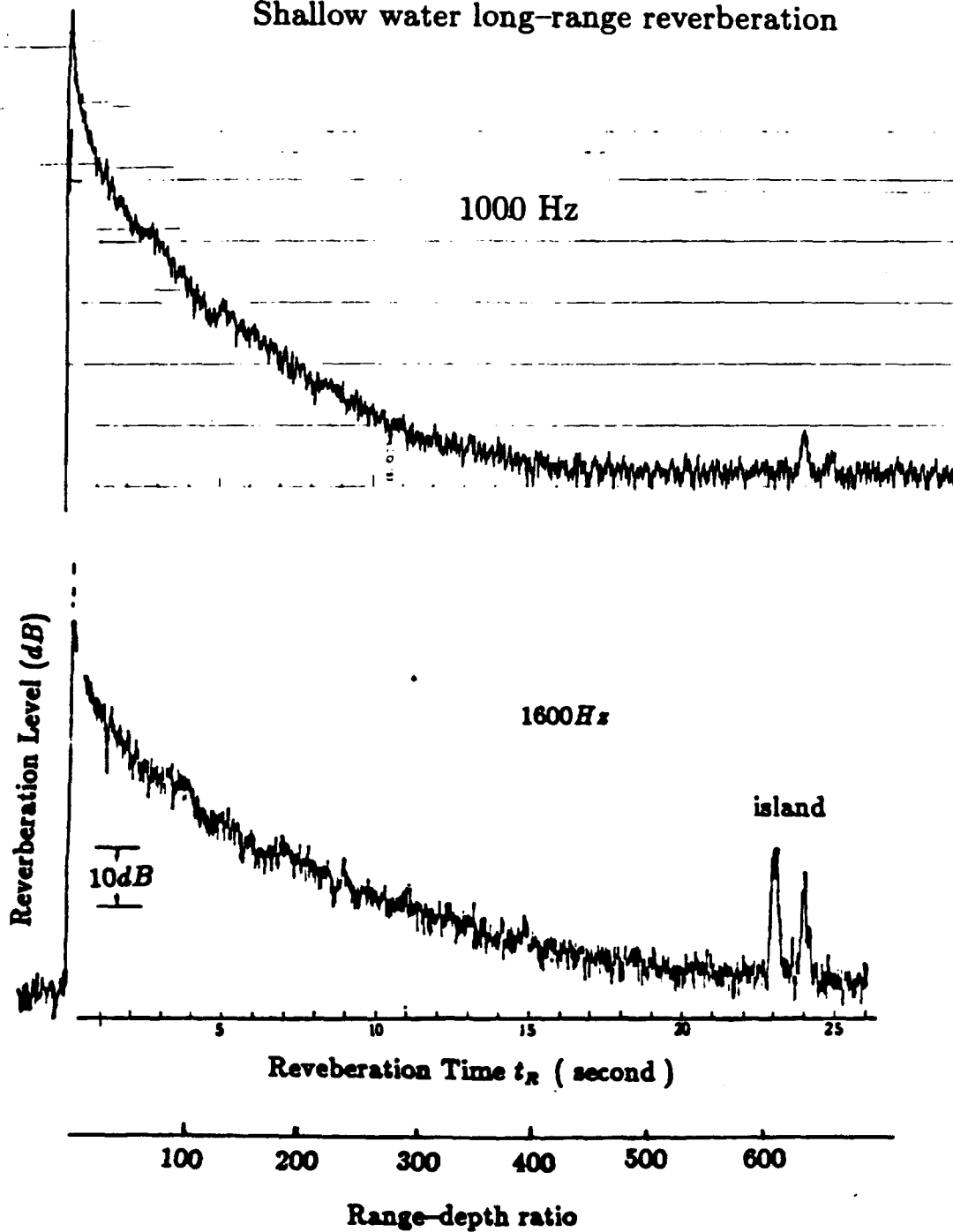
Thanks !

Nonreciprocity of Long-range Reverberation in a Wedged Continental Shelf

J. Z. Zhou, X. Z. Zhang, P. H. Rogers and D. H. Guan

- 1. Background (The shallow water reverberation problem seems to fall into “an endless loop” with no way out.)**
- 2. Averaged angular power spectrum method for long-range reverberation in shallow water.**
- 3. Transformation relation → Bottom scattering at small grazing angles, derived from experimental reverberation data.**
- 4. The WKB approximation → adiabatic mode theory.**
Reverberation in a wedged shallow water is not reciprocal.

Shallow water long-range reverberation



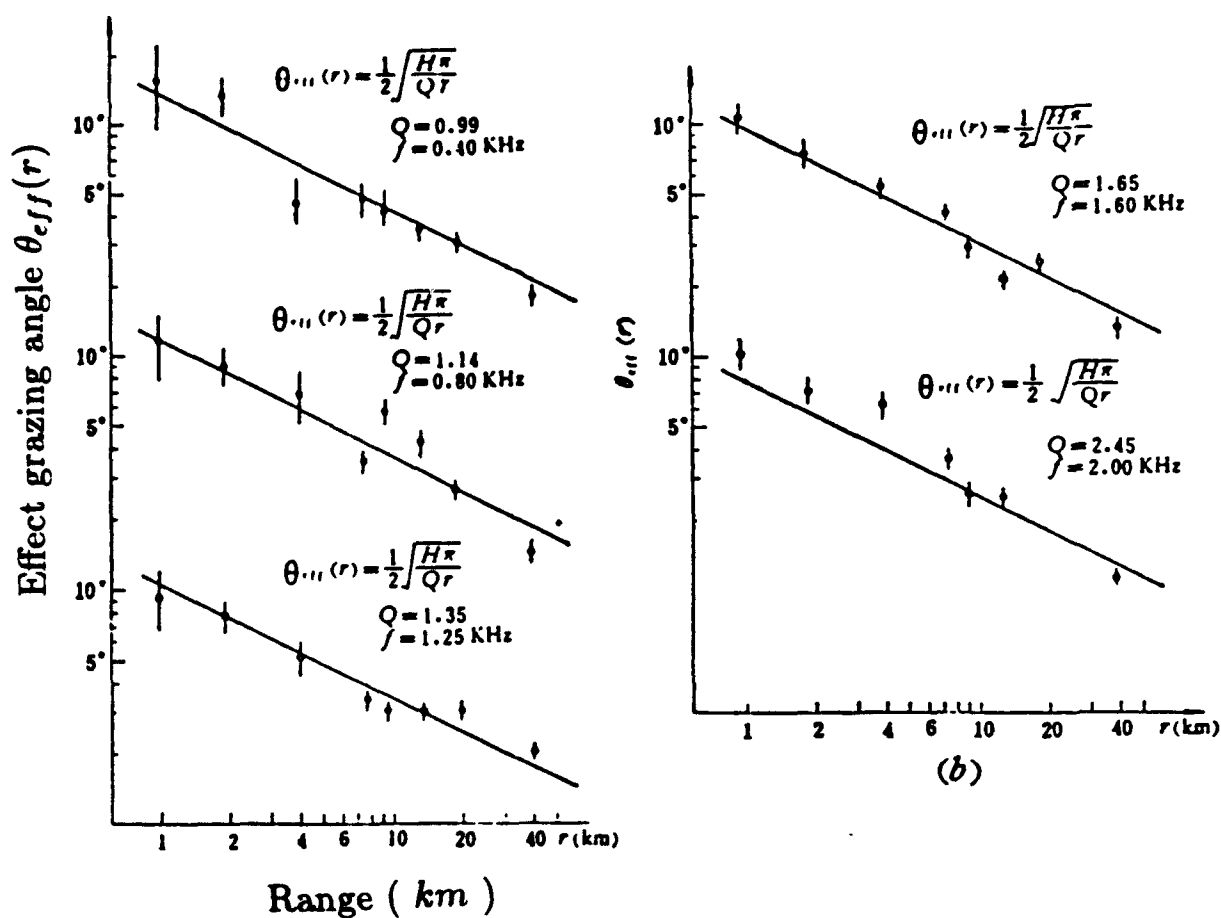
$$\theta_{eff}(r) = \frac{1}{2} \left(\frac{\pi}{Q} \right)^{1/2} \left(\frac{H}{r} \right)^{1/2} \quad (1)$$

$$-\ln|V(\theta)| = Q\theta$$

Q - the bottom reflection loss parameter at small grazing angle θ

The Vertical coherence of sound propagation in Pekeris model (Smith, Zhou)

$$\rho(r, d) = e^{-\frac{H}{4Q} k^2 d^2} = e^{-\frac{k^2 d^2}{\pi} \theta_{eff}^2(r)}$$



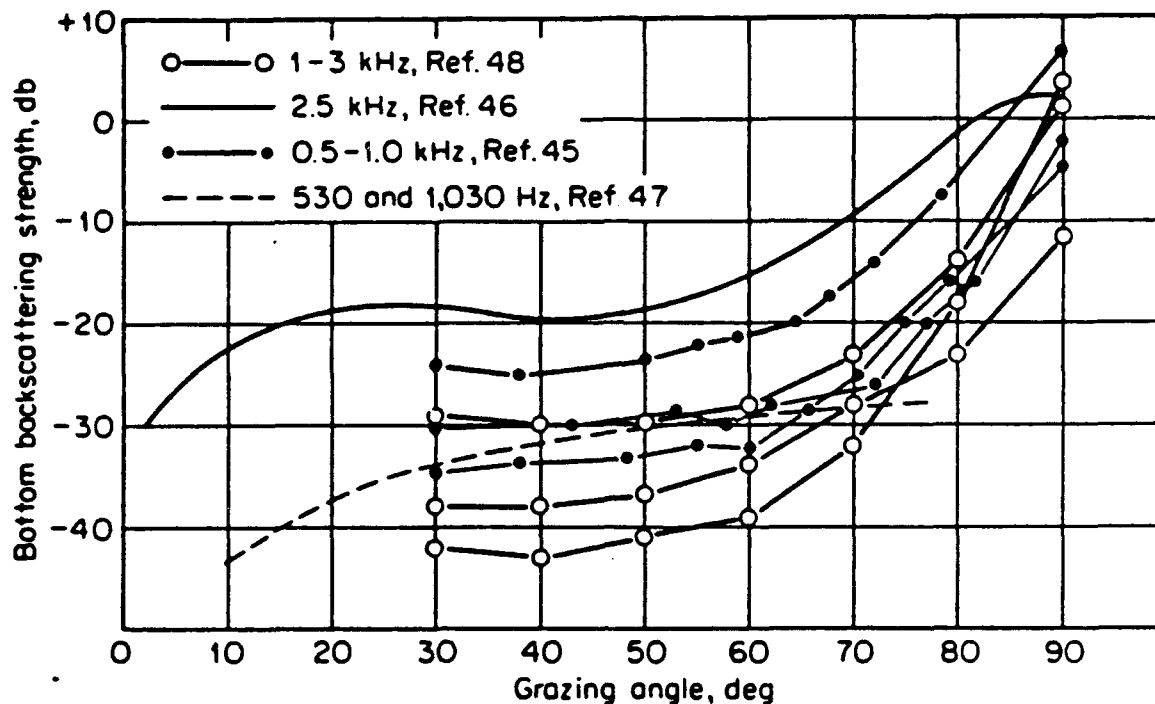


FIG. 8-22. Low-frequency deep-water bottom backscattering strength as reported in four sets of measurements.

Shallow Water Acoustics Workshops Proceedings (1983) :

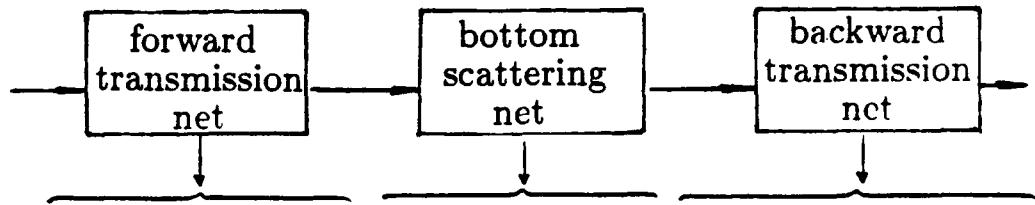
"Grazing angles of primary importance to shallow water applications range from about 30° to near 0° with the smaller angles being more important..... To date, NOVOCEANO has not been able to report either bottom reflectivity or bottom backscattering values for any shallow water area. "

Brekhovskih, Zhou
Smith
Weston

$$\begin{aligned}
 I(r, z; z_0) &= \frac{2}{r} e^{-\alpha r} \int \frac{2e^{\frac{2\ln|V(\theta)|}{s} r}}{S \tan \theta(z)} d\theta(z_0) \\
 &= \frac{2e^{-\alpha r}}{Hr} \int I_{aps}(\theta, r, z; z_0) d\theta
 \end{aligned} \tag{2}$$

$I_{aps}(\theta, r, z; z_0)$ - the angular power spectrum;

Boudary condition + sound velocity profile \rightarrow a angular filter of sound propagation.



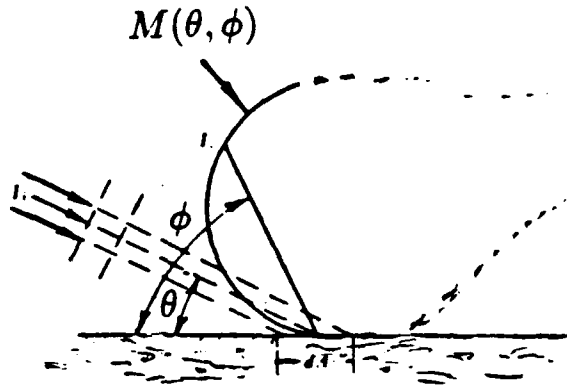
$$R(r, z; z_0) = \int \int \frac{e^{-\alpha r}}{Hr} I_{aps}(\theta, r, z') * A * M(\theta, \phi) * \frac{e^{-\alpha r}}{Hr} I_{aps}(\phi, r, z') d\theta d\phi \tag{3}$$

where the $M(\theta, \phi)$ is the scattering coefficient of plane wave from bottom.

$$M(\theta, \phi) = ?$$

It must be a very complex function of bottom surface roughness, sediment type, sediment inhomogeneity, angle, frequency and so on. Unknown ! No way out ?

Arbitrary angle dependence of equivalent bottom scattering:



Reasonable assumptions at small grazing angles

- 1) Decreasing function of angle with decreasing grazing angle;
- 2) Reciprocal when incident angle and backward scattering angle exchange, i.e., $M(\theta, \phi) = M(\phi, \theta)$

$$M(\theta, \phi) = \left(\sum_i^N \sqrt{\mu_i} \Delta_i(\theta) \theta^{n_i} \right) * \left(\sum_i^N \sqrt{\mu_i} \Delta_i(\phi) \phi^{n_i} \right) \quad (4)$$

where

$$\Delta_i(x) = \begin{cases} 1, & \text{if } x \in [x_{i-1}, x_i]; \\ 0, & \text{otherwise.} \end{cases} \quad (5)$$

In the Pekeris model the angular power spectrum

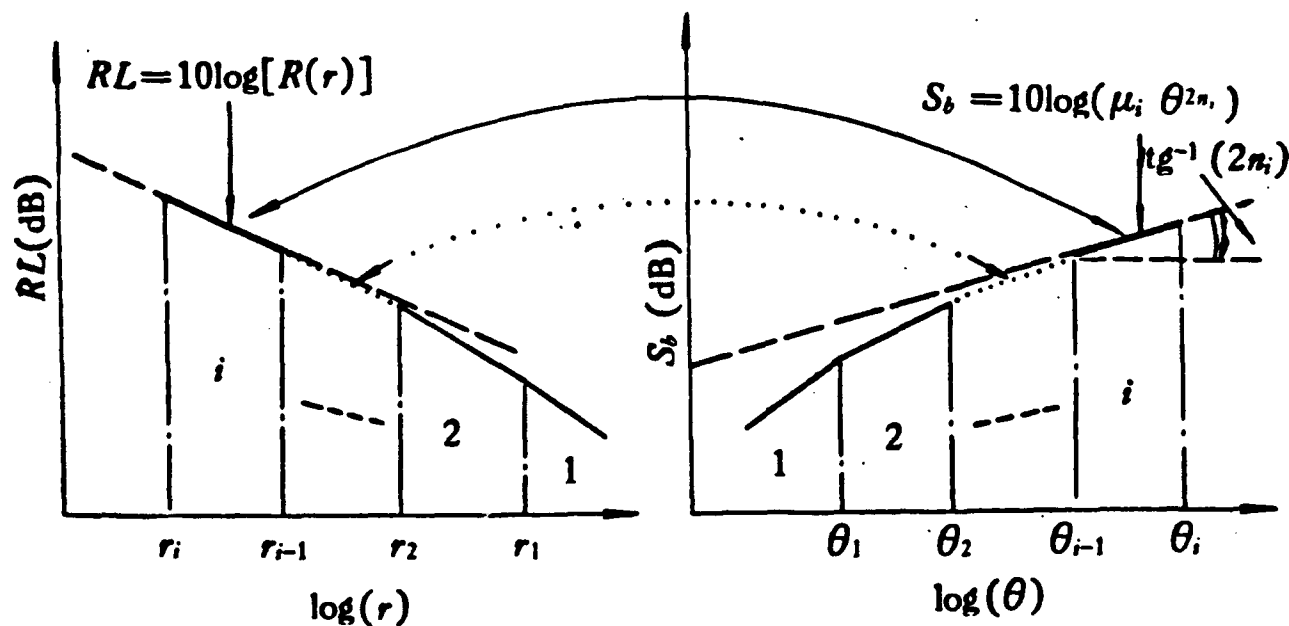
$$I_{aps}(\theta, r) = e^{-\frac{Qr}{H}\theta^2} \quad (6)$$

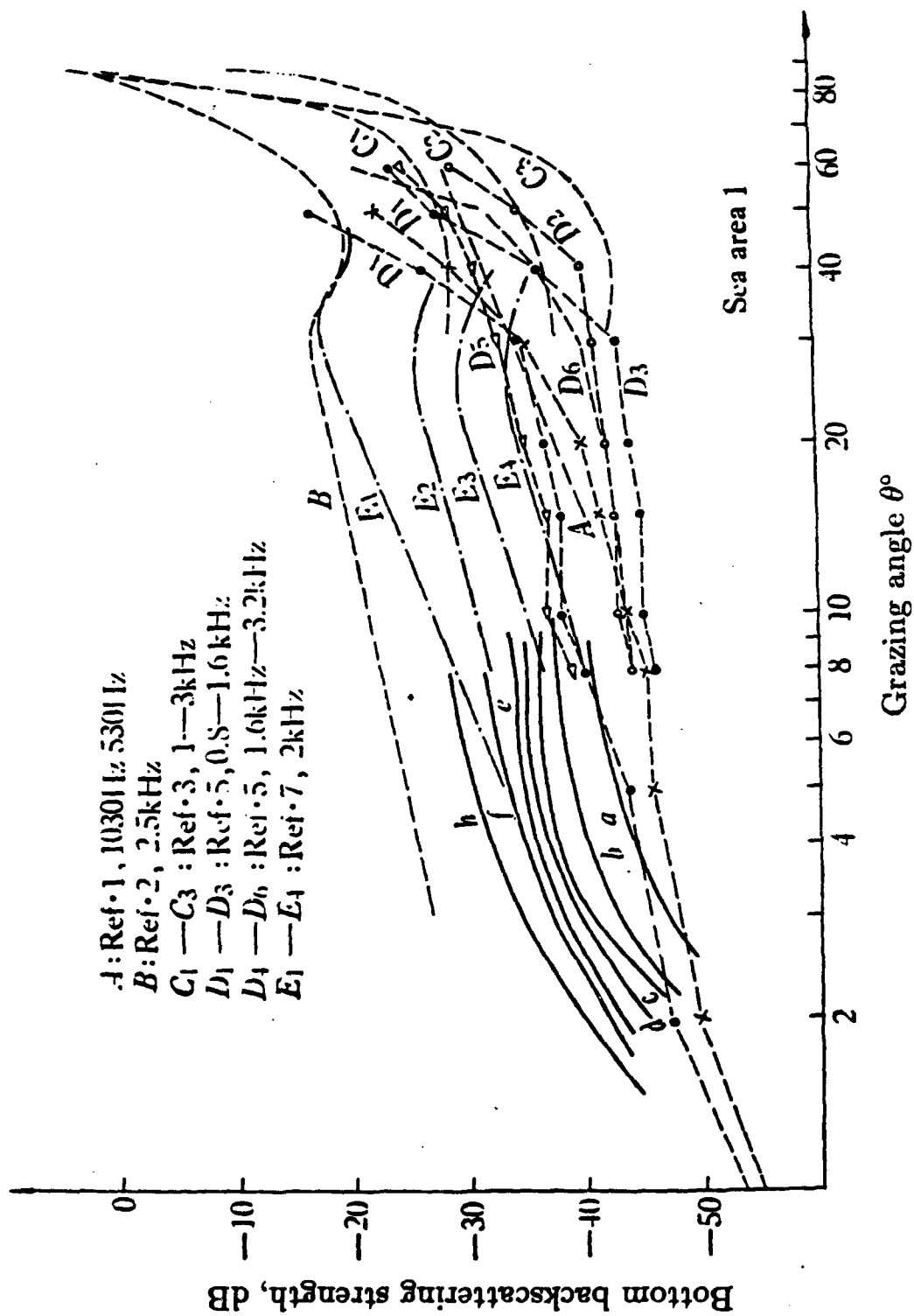
From Eqs.(3-6), we get an expression for long-range reverberation as

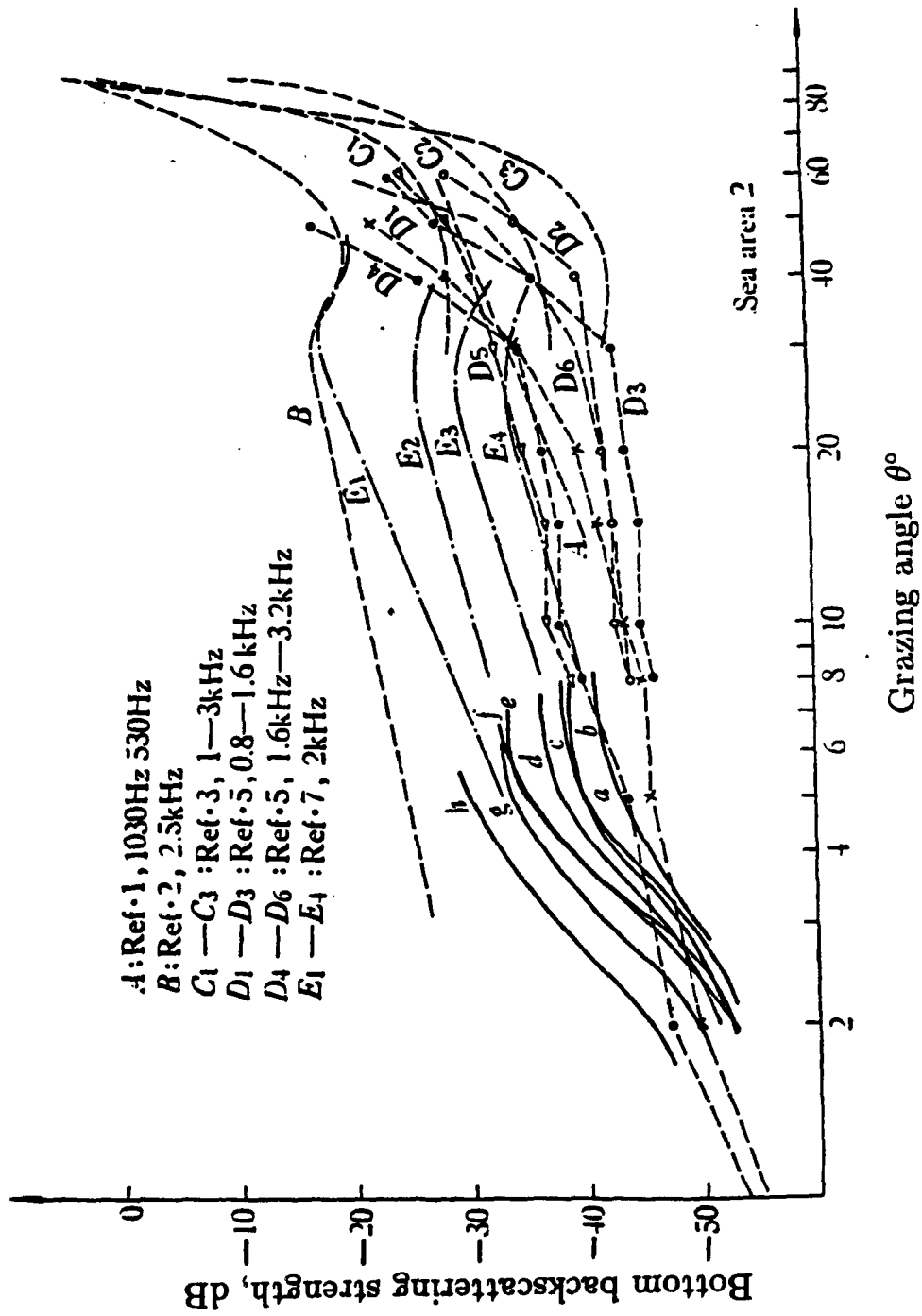
$$R(r) = e^{-2\alpha r} \sum_i^N R_i * \Delta_i(r) \quad (7)$$


$$R_i(r) = \frac{\mu_i \pi c T}{(n_i + 1)^2} * \frac{1}{H^{(1-n_i)} Q^{(1+n_i)}} * \frac{1}{r^{(2+n_i)}} \quad (8)$$

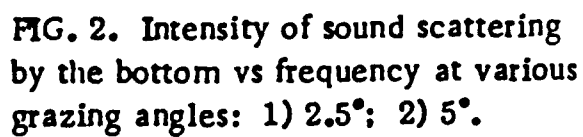
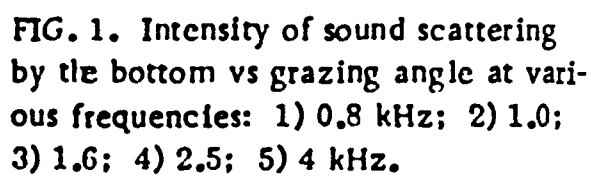
Transformation relation between the range dependence of RL
and the angular dependence of bottom scattering:







Our data { 



In shallow water of variable depth, the an adiabatic normal mode expression (**Pierce**) :

$$P(r, z; z_0) = \sqrt{\frac{2\pi}{r}} e^{-i\frac{\pi}{4}} \sum \frac{1}{\sqrt{k_m(r)}} \psi_m(0, z_0) \psi_m(r, z) \exp \left[-i \int_0^r K_m(u) du \right] \quad (9)$$

where

$$K_m^2(r) = k_m^2(r) + A_{mm}(r) \approx k_m(r) \quad (9a)$$

$$A_{mm} = \int \left(\psi_m \frac{\partial^2 \psi_m}{\partial r^2} \right) dz \quad (9b)$$

The adiabatic mode theory means that the local modes adapt to local environment. So the grazing angle of equivalent ray of normal modes satisfy

$$k_m(r) = k(r) \cos(\theta_m(r)) \quad (10)$$

$$H(r) \sin \theta_m(r) = H(0) \sin \theta_m(0) \quad (11)$$

For a wedged homogeneous continental shelf the water depth can be expressed by

$$H(r) = H(0) (1 + ar) \quad (12)$$

Applying WKB approximation we have the averaged sound intensity :

$$I(r) = \frac{2}{H(0)r} \int \exp \left[\int_0^r \frac{L_n |V(\theta_m)|}{H(r)} \tan(\theta_m(r)) dr \right] d\theta_m(r) \quad (13)$$

The averaged angular power spetrum

$$I_{ps}(\theta, r) = e^{\int_0^r \frac{L_n |V(\theta_m)|}{H(r)} \tan(\theta_m(r)) dr} \quad (14)$$

The averaged intensity of sound propagation is:

$$I(r) = \sqrt{\frac{2\pi}{Q[H(0) + H(r)]}} * \frac{1}{r^{3/2}} \quad (15)$$

The averaged reverberation intensity is:

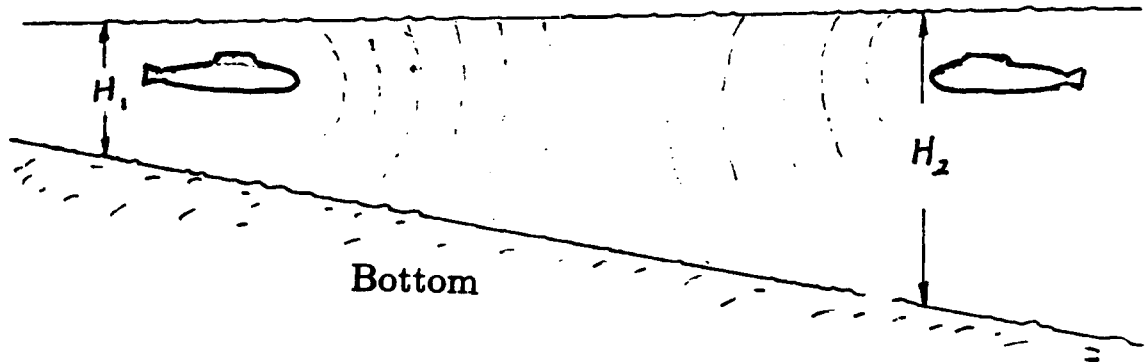
$$R(r) = \frac{\mu\pi^{(2-n/2)}c\tau}{4} \frac{H^n(0)}{[Q \frac{H(0)+H(r)}{2}]^{(1+n/2)}} \frac{1}{r^{(2+n/2)}} \quad (16)$$

Sound propagation is reciprocal if we exchange the positions of the source or receiver. But the monostatic reverberation intensities, obtained at two terminations with a depth of H_1 or H_2 , would not be reciprocal.

$$\frac{R_{H_1}(r)}{R_{H_2}(r)} = \left(\frac{H_1}{H_2}\right)^N \quad (17)$$

where N is the angular index of bottom backscattering defined as

$$BS(\theta) = 10 \log_{10} (\mu \sin^N \theta) \quad (18)$$



If $H_1 = 50m$, $H_2 = 200m$, $N = 2$, then the reverberation interference at shallower area would be 12dB less.



THE EFFECTS OF INTERNAL SOLITONS OR BOTTOM RELIEF ON SOUND PROPAGATION IN SHALLOW WATER

Xue-zhen ZHANG and Ji-xun ZHOU

Institute of Acoustics, Academia Sinica, P.O.Box 2712, Beijing 100080, People's Republic of China and School of Mechanical Engineering, Georgia Institute of Technology, Atlanta, GA 30332, USA

Peter H. ROGERS

School of Mechanical Engineering, Georgia Institute of Technology, Atlanta, GA 30332, USA

Introduction

Strong bottom interaction, variable media and multipath propagation make shallow water acoustics very challenging. One of unexplained phenomenon for shallow water sound propagation, in the contrast with the so-called the optimum propagation frequency, is that high acoustic propagation loss over some frequency range is frequently reported¹⁻³. Weston attributes such a phenomenon to fish activities¹. In some case it is associated with sediment shear-wave resonances within the layer of sediment². Fig. 1 shows a frequency response for shallow-water sound propagation in the summer (with a strong thermocline shown in Fig.

2) in the Yellow Sea off China, obtained by Zhou and his group at the IAAS³. Around 600 Hz and above 1100 Hz the transmission loss is abnormally large. Several years of observations, all made in August at the same area with a similar strong thermocline, have shown that the frequency responses of sound propagation is often a strong function of both time and propagation direction. The variability of the high loss frequency range and the apparent anisotropic characteristics of sound propagation occur with no obvious explanation in terms of fish swim bladder resonance. For the strong thermocline shown in Fig. 2, if both sound source and receiver are located beneath the thermocline, the sea surface influence on the long-range sound field (or lower modes) is negligible. While it might be possible that one could use the Weston fish model (or some other model) to quantitatively match the experimental data, we consider the possibility that the acoustic normal-mode conversion caused by internal soliton or bottom relief packets may also explain the data.

Ocean models

1. *Internal soliton packets.* Our numerical results have shown³ that the acoustic mode-coupling induced by internal wave packets with a gated sine waveform (model I) exhibits frequency, soliton wavelength and packet length resonances. The interaction between the acoustic waves and internal wave packets could provide a plausible explanation for

COLUMN SPACE: JOURNAL OF THE INSTITUTE OF ACOUSTICS

Sta

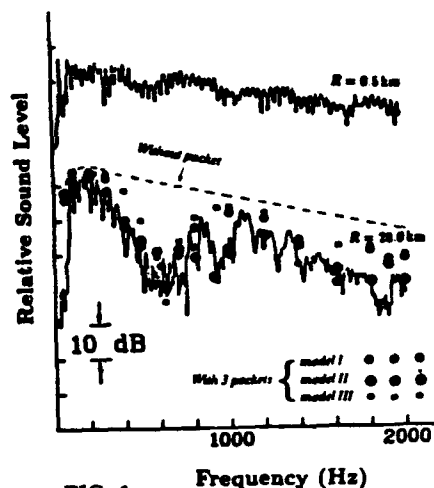


FIG. 1.

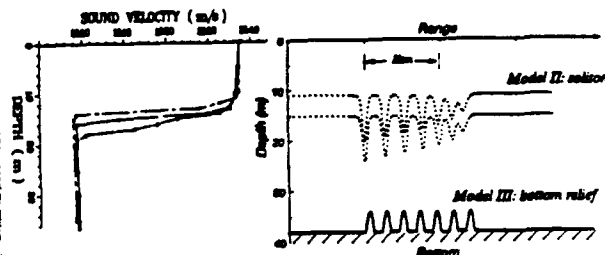


FIG. 2.

the observed anomalous propagation in the summer. Now we extend the model to consider the influence of the characteristic properties of more realistic oceanic soliton packets.

Solitons in shallow water ($h/\lambda_s \ll 1$) are described to first order in wave amplitude by the Korteweg-de Vries (KdV) equation: $A_t + C_0 A_x + \mu A A_x + \delta A_{xxx} = 0$. A solution to this equation is $A(x - \alpha) = a \operatorname{sech}^2(\frac{x - \alpha}{L})$. The density (temperature) profiles corresponded to Fig. 2 is very reasonably described by a two-layer fluid model. The soliton phase speed c and wavelength λ_s (and scale parameter L) are then easy to obtain. When the initial solitary wave propagates, it often evolves more rank-ordered solitons and exhibits clear nonlinear features. Instead of the previous simple gated sine function, three packets with typical characteristics of internal solitons are used: the classical sech^2 soliton shape which decreases in wavelength and amplitude toward the rear of the packet (Model II, shown in Fig. 2).

2. *Bottom relief group.* For simplicity, we assume that an undulating seabed can be expressed by a half sine function, shown in Fig. 2 (Model III).

Approach

The presence of internal soliton or bottom relief packets makes the environmental parameters range dependent. The parabolic equation (PE) model is used to numerically simulate the effect of internal soliton packets or bottom relief

groups on sound propagation in shallow water. We arbitrarily put three packets of solitons or bottom relief located at 5 km, 15 km and 25 km along propagation track. The PE method⁴⁻⁵ is used to calculate the frequency response of acoustic transmission loss. When analyzing the characteristics of acoustic mode-coupling, we put just a single group of solitons or bottom relief at 15 km and use the first normal mode alone as the initial input field to the PE code (IFD). The acoustic field obtained using PE model is decomposed into the normal modes. The results are compared with mode-coupling theory⁶⁻⁸ in order to improve our understanding of how mode conversion acts to become an important mechanism of acoustic attenuation in shallow water.

Results and discussion

1. Similar to model I and model III, internal wave packets with the classic characteristic properties of soliton could also cause abnormally large attenuation for acoustic propagation in shallow water. The differences between the results with and without the soliton packets is shown in Fig. 1 by ••••.

2. The interaction of sound waves with soliton or bottom relief group exhibits (signal) frequency, (radial inhomogeneity) wavelength and packet length resonances. As an example, the bottom relief wavelength and group length resonances are shown in Fig. 3 ($f = 630\text{Hz}$, $r = 30\text{km}$).

3. For a shallow water with a strong thermocline the apparent resonance interaction of sound waves with three ocean models could only occur under a specific circumstance: when the acoustic mode coupling caused by environmental parameter variation transfers a significant amount energy from lower mode into higher-order modes with much larger attenuation rate. For example, the PE field at 18km is decomposed to normal modes with the results shown in Fig. 4 ($f = 630\text{Hz}$, $r = 18\text{km}$). Apparently, after the interaction of the first mode with a packet at 15km a significant amount energy has been coupled into higher-order modes.

4. The "resonancelike" behavior of transmission loss predicted by the PE analysis is consistent with mode coupling theory. Significant energy transfer will occur between mode m and n if $k_{in,h} \approx k_m - k_n$, here $k_{in,h}$ is the wave number of the spectrum peak of the radial inhomogeneity. The mode coupling is a periodic (resonance) function of the soliton (or relief) group length.

5. The main intention of this work is to show what would happen to sound propagation if soliton or bottom relief packets are present, not to solve an inversion problem for internal waves or to determine sound propagation for a specific area. It is expected that any abnormal attenuation for sound propagation in a real shallow water environment might be caused by any combination of several different mechanisms, internal wave(or bottom relief) interaction must be considered as one such mechanism.

ACKNOWLEDGMENTS: Work Supported by the IAAS and ONR, USA.

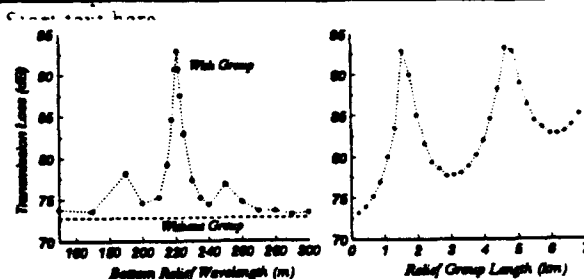


FIG. 3.

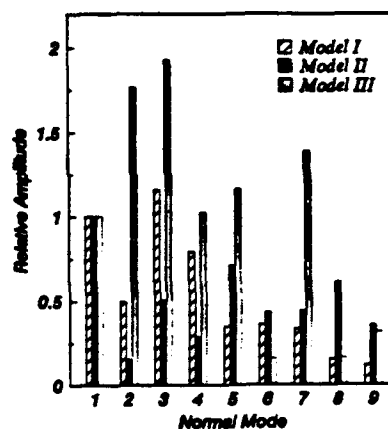


FIG. 4.

REFERENCES

1. W. E. Weston, *J. Sound Vib.* **18**, 499-510(1971).
2. S. J. Hughes, D. D. Elis, D. M. F. Chapman and P. R. Staal, *J. Acoust. Soc. Am.* **88**, 283-297(1990).
3. J. X. Zhou, X. Z. Zhang and P. H. Rogers, *J. Acoust. Soc. Am.* **90**, 2042-2054(1991).
4. D. Lee and G. Botseas, Naval Underwater Systems Center, New London, CT (1982), TR No.6659.
5. G. Botseas, D. Lee and K. E. Gilbert, Naval Underwater Systems Center, New London, CT (1983), TR No.6905.
6. L. B. Dozier and F. D. Tappert, *J. Acoust. Soc. Am.* **63**, 353-365(1978).
7. S. T. McDaniel and D. F. McCammon, *J. Acoust. Soc. Am.* **82**, 217-223(1987).
8. S. T. McDaniel, *J. Acoust. Soc. Am.* **72**, 916-923(1982).

Resonant interaction of sound wave with internal solitons in the coastal zone

Ji-xun Zhou and Xue-zhen Zhang

Institute of Acoustics, Academia Sinica, Beijing 100080, People's Republic of China and School of Mechanical Engineering, Georgia Institute of Technology, Atlanta, Georgia 30332

Peter H. Rogers

School of Mechanical Engineering, Georgia Institute of Technology, Atlanta, Georgia 30332

(Received 20 February 1991; accepted for publication 30 May 1991)

Naturally occurring internal solitary wave trains (solitons) have often been observed in the coastal zone, but no reported measurements of such solitary waves include low-frequency long-range sound propagation data. In this paper, the possibility that internal waves are responsible for the anomalous frequency response of shallow-water sound propagation observed in the summer is investigated. The observed transmission loss is strongly time dependent, anisotropic and sometimes exhibits an abnormally large attenuation over some frequency range. The parabolic equation (PE) model is used to numerically simulate the effect of internal wave packets on low-frequency sound propagation in shallow water when there is a strong thermocline. It is found that acoustic transmission loss is sensitive to the signal frequency and is a "resonancelike" function of the soliton wavelength and packet length. The strong interaction between acoustic waves and internal waves, together with the known characteristics of internal waves in the coastal zone, provides a plausible explanation for the observed anomalous sound propagation in the summer. By decomposing the acoustic field obtained from the PE code into normal modes, it is shown that the abnormally large transmission attenuation is caused by "acoustic mode-coupling" loss due to the interaction with the internal waves. It is also shown that the "resonancelike" behavior of transmission loss predicted by the PE analysis is consistent with mode coupling theory. As an inverse problem, low-frequency acoustic measurements could be a potential tool for remote-sensing of internal wave activity in the coastal zone.

PACS numbers: 43.30.Bp, 43.30.Ft, 43.25.Cb

INTRODUCTION

Naturally occurring internal wave packets have often been observed in the coastal zone, especially in the summer. The mechanism for the generation of these nonlinear internal waves have been widely investigated in the geophysics and fluid mechanics community. Unfortunately, however, no reported measurements of such solitary waves include low-frequency long-range sound propagation data. The acoustic community has paid little attention to the effect of solitary waves on sound propagation with the exception of the work of Baxter and Orr that was based on ray theory and calculated the influence of an oceanic internal wave packet on short-range (high-frequency) sound propagation.¹ Experiments, conducted by Zhou and his group at Institute of Acoustics of the Chinese Academy of Sciences in Beijing over a four-year period at the same area of Yellow Sea, have shown that the frequency response of shallow water sound propagation in the summer is a strong function of time and propagation direction, and sometimes exhibits an abnormally large attenuation over some frequency range. A part of these results was reported before,^{2,3} but it cannot be explained by a conventional range-independent model of sound propagation using reasonable bottom acoustic parameters and an average sound-speed profile.

In this paper, we investigate the possibility that the anomalous propagation results are due to the presence of

internal waves. First, we briefly discuss the characteristics of internal wave packets in the coastal zone. We then review the aforementioned experimental results of Zhou *et al.* that exhibited the anomalous frequency response. In Sec. III, we hypothesize that this anomalous, anisotropic frequency response is caused by the influence of internal wave packets. We support the hypothesis with numerical simulation results obtained using the parabolic equation (PE) propagation model. In Sec. IV, we decompose the acoustic field obtained by using the PE model into the normal modes, and show that the abnormally large transmission loss which occurs over certain frequency ranges is due to "mode-coupling" loss induced by the internal wave packets. In Sec. V, we show that "resonancelike" behavior of the attenuation is consistent with mode coupling theory.

I. CHARACTERISTICS OF INTERNAL WAVE PACKETS IN THE COASTAL ZONE

Internal waves have been observed almost everywhere in the ocean.⁴ In the open ocean they are best described as a stochastic phenomenon with a broadband frequency wave number spectrum.⁵ However, analysis of extensive data on internal waves in the coastal zone,⁶⁻²² has shown that these waves exhibit the properties of solitons. The experimental data includes: current and temperature measurements; vertical profiles from CTD, XBT, and acoustic echo sounding

devices; ship's radar and satellite (or space shuttle) images obtained at optical and radar frequencies. We are primarily interested in the effect of internal solitons on long-range sound propagation in the coastal zone, and not the mechanisms for the generation or propagation of internal wave packets (which has been widely investigated in the geophysics and fluid mechanics communities). We thus limit our discussion of internal waves to the following summary of the relevant characteristics of internal wave packets in the coastal zone.

(1) Internal waves in shallow water are frequently observed in deterministic groups (wave packets) with well-defined wavelengths that are describable as solitary waves (or solitons). These waves are usually observed in summer when they are trapped in a strong and shallow seasonal thermocline.

(2) Solitons in shallow water ($h/\lambda \ll 1$) are described to first order in wave amplitude by the Korteweg-de Vries (KdV) equation: $A_t + C_0 A_x + \mu A A_x + \delta A_{xxx} = 0$. The solitary waveforms often have a "sech²" profile. When an initial solitary wave propagates, it often evolves more rank-ordered solitons and exhibits clear nonlinear and dispersive features such as higher-than-linear group velocity, and a decrease in wavelength and amplitude toward the rear of the packet.

(3) The number of wave packets are highly correlated with the strength of the local tides: The maximum number occurs during spring tides and the minimum number occurs during neap tides. Whether or not they occur is critically dependent on the structure of the background shear and stratification profiles.

(4) Solitary wave packets propagate shoreward, and are often generated by a tidally driven flow over sills, continental shelf edges, or other major variation in underwater topography.

(5) Because of the shallowness of the summer seasonal thermocline and the large amplitude of the coastal internal waves, strong surface expressions of solitons have been observed with a variety of remote sensors, including photographs and synthetic aperture radar (SAR) from satellites and space shuttles.

Naturally occurring large-amplitude internal solitons

have been reported in many coastal zones of the world such as: the Massachusetts Bay,^{6-8,11} the New York Bight,²⁰⁻²² Gulf of California,^{10,13} Andaman Sea offshore Thailand,^{9,18} the Australian North West Shelf,¹⁹ the Sulu Sea between the Philippines and Borneo,^{15,16} off the coast of Portugal,^{12,18} off Hainan Island in the South China Sea and off the Strait of Gibraltar in Alboran Sea,²³ the Scotian Shelf off Nova Scotia,¹⁴ the Celtic Sea,¹⁷ and so on. They have also been observed in lakes.^{24,25} As an example, an excellent record of an internal wave packet is shown in Fig. 1. It was obtained by Orr using high-frequency acoustic scattering in the Massachusetts Bay.^{7,8} The period of the waves is Doppler shifted by the ship's speed of about 2.5 kn. The seasonal thermocline is displaced by 30 m (arrow 1) and the stratified point scatterers (zooplankton?) at 30 to 40 m are displaced more than 20 m (arrows 2 and 3). The heavy acoustic backscattering in the vicinity of arrow 4 and extending in an oscillatory pattern throughout the figure is possibly caused by turbulent mixing in the thermocline. The heavy scattering near 75 m is probably caused by euphausiid and mysid shrimp. Figure 2, taken from the work of Osborne and Burch,⁹ shows how rough and smooth bands on the water surface can be caused by internal solitons. Such surface expressions have been detected by ship, satellite, and space shuttle in many areas. For example, Fig. 3, taken from the work of Liu,²¹ is a line drawing of the internal wave packets in the New York Bight, observed from Seasat satellite, which clearly illustrates the anisotropic characteristics of internal waves in the coastal zone. There are numerous wave groups, all propagating shoreward. Each group consists of many solitons. The number of groups often depends on the local tide strength and the density profile of water column, i.e., it is a function of time.

The characteristics of internal wave packets in the coastal zone summarized here, will be helpful in explaining the anomalous experimental results, introduced in the next section.

II. FREQUENCY RESPONSE OF SHALLOW-WATER SOUND PROPAGATION IN THE SUMMER

Zhou and his group at Institute of Acoustics, Academia Sinica (IAAS) have measured the frequency response of shallow-water sound propagation under the condition of a

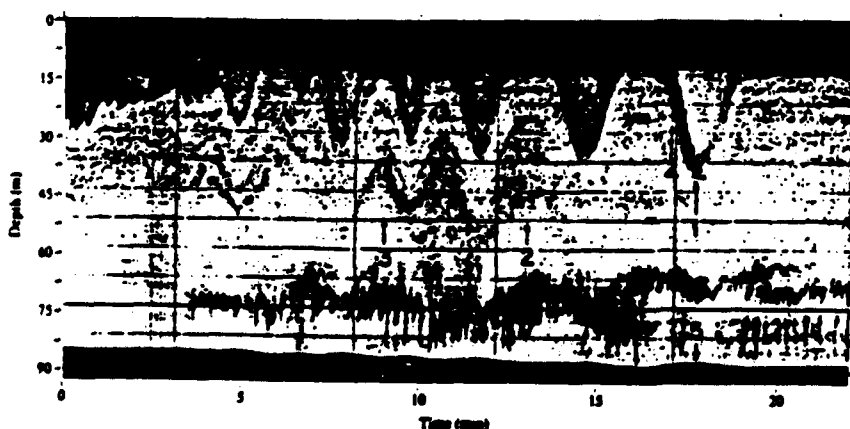


FIG. 1. A 200-kHz acoustic record of an internal wave packet observed in the Massachusetts Bay.

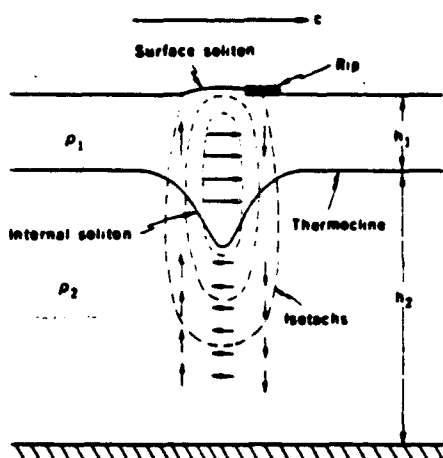


FIG. 2. A sketch of an internal soliton in a two-layer fluid model showing the fluid-particle velocities and the surface expression.

strong thermocline in the Yellow Sea off China. A great deal of data was collected over several years in the same area, (which had a characteristically flat seabottom with high-speed sediments). The data included measurements of sound propagation, long-range reverberation, sound field spatial coherence and utilized normal-mode spatial filtering techniques. The acoustic parameters of the bottom for this area were obtained by wideband acoustic measurements.^{26,27} Generally speaking, the experimental data fits theoretical predictions very well. For example, transmission losses as a function of frequency for winter, late spring, and sometimes for summer were correctly predicted. However, it was found that, in the summer, even along the same experimental track, with similar averaged sound-speed profiles the

frequency response of sound transmission could often be very different for different years.

Figure 4 shows power spectra that are obtained by averaging several explosive propagation signals. The upper curve is the power spectrum at a propagation range of 0.5 km, the lower one is at a range of 28 km. The difference between the two curves is a measure of the sound transmission loss between two receiving points, i.e., the frequency response of sound propagation. Between 300 and 1100 Hz, especially around 600 Hz, the transmission loss is abnormally large. The measured sound-speed profiles at the receiving ship are shown in Fig. 5. Both source and receiver were located below the thermocline. The anomalous transmission loss cannot be explained by conventional models of sound propagation (with a full complement of bottom acoustic parameters and an averaged sound-speed profile of water column). In order to explain this phenomenon, Zhou and his colleagues at IAAS made observations, every August for 4 years at same area. The abnormal attenuation frequency range varied with time. In Fig. 4, it occurs at around 600 Hz, but for different years or different propagation directions, it has been observed around 500, 1200, or 1600 Hz. Sometimes, there is no apparent abnormal attenuation frequency range.

In another experiment, the frequency response at a fixed range for six different radial directions was obtained. The results are shown in Fig. 6. The transmission distance was kept constant at 28 km, by moving the source ship along one quadrant of a circle centered at the receiving ship. Each curve represents an averaged value obtained from several explosive signals. Transmission loss is obviously a strong function of propagation direction. For different propagation directions, at some frequencies, the sound intensity varied as much as 25 dB! However, in another experiment, at the same

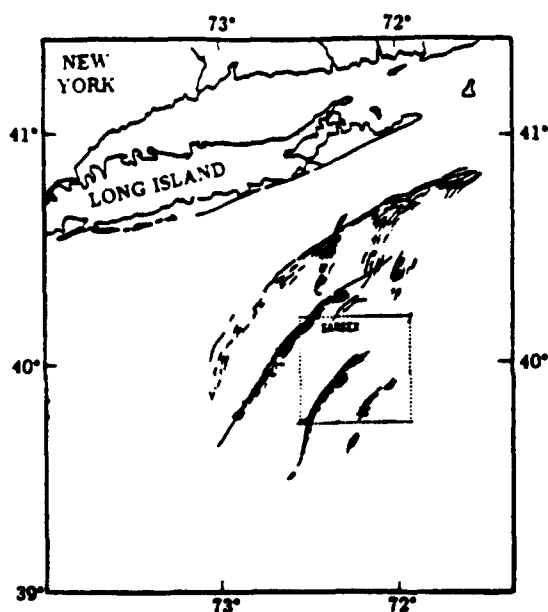


FIG. 3. Line drawing indicating internal wave packets in the New York Bight, observed from the Seasat satellite.

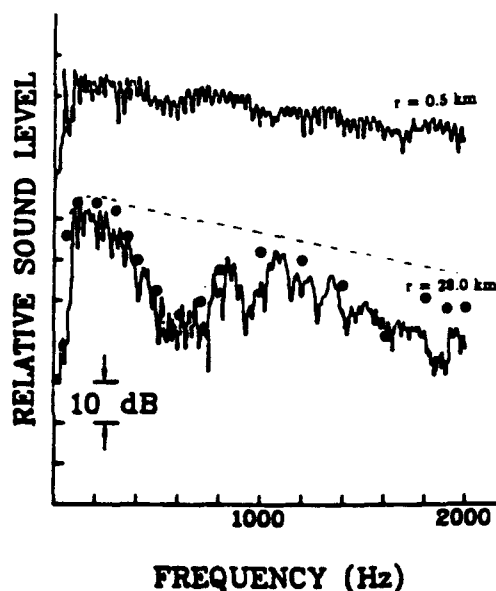


FIG. 4. Explosive signal power spectrum for shallow-water sound propagation in the summer which exhibits an abnormally large attenuation around 600 Hz (experimental data). Both source and receiver are located below the thermocline. Computational results (see Sec. III B): (1) without packet — — — (2) with three packets $\circ \circ \circ$.

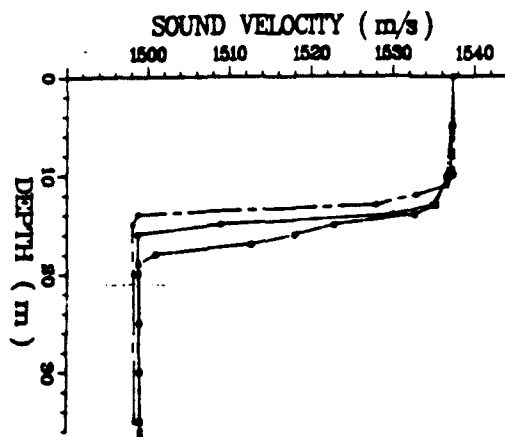


FIG. 5. Three sound-speed profiles measured at the receiving ship at different times.

place, in a different year, two orthogonal propagation directions were observed to have almost identical frequency responses. It was not at all clear why, when there is a strong thermocline, the frequency response of shallow-water sound propagation in the experimental area was often observed to be a strong function of both time and propagation direction, and sometimes exhibited abnormally large attenuation over some frequency range.

Using ray theory and experimental contours of sound speed versus range and depth, Baxter and Orr¹ calculated the influence of an internal wave packet on short range

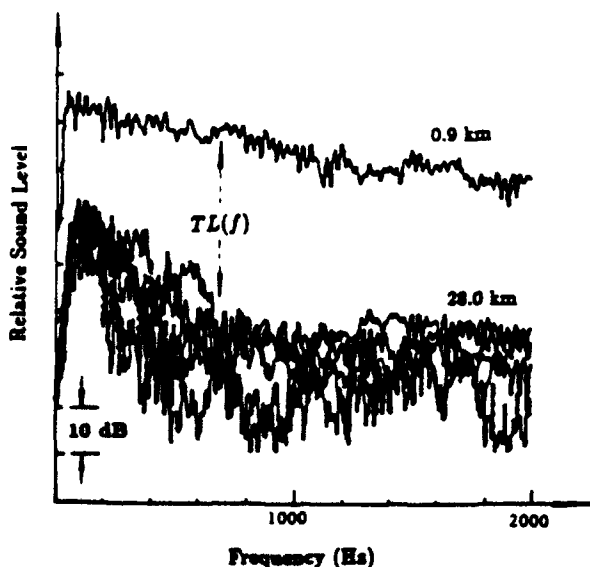


FIG. 6. Frequency response of sound transmission loss (TL) for the summer which shows different results for different propagation directions.

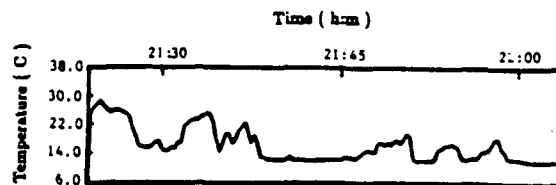


FIG. 7. A record of temperature versus time over a period of 42 min at a fixed depth (near the thermocline).

(high-frequency) sound propagation. The calculations showed that at a fixed position the intensity of sound field could vary by as much as 20 dB, relative to a case without the presence of the internal wave packet. We hypothesized that internal wave packets might have a strong influence on low-frequency long-range sound propagation in shallow water as well and could possibly explain Zhou's Yellow Sea propagation data. In the next section, we support this hypothesis with numerical simulation results obtained using the parabolic equation method.

III. NUMERICAL SIMULATION OF THE INFLUENCE OF INTERNAL WAVE PACKETS ON SOUND PROPAGATION

A. Oceanic model

The presence of internal waves makes the sound-speed profile of the water range dependent. Unfortunately, in Zhou's experiments there were no accompanying systematic measurements of the internal wave field; and only the sound-speed profile at the receiver was measured. During the time period over which the frequency response shown in Fig. 4 was obtained, it was found that the thermocline depth at receiving ship location did change with time. Figure 5 shows three sound-speed profiles that were obtained at different times.

During the experiment, Zhang²⁸ measured the temperature fluctuation as a function of time at the receiving ship. A record of temperature fluctuations over a period of 42 min at a fixed depth (around the thermocline) is shown in Fig. 7. The temperature fluctuated between about 13 °C and 27 °C. The possible presence of several individual solitary waves is indicated by temperature peaks due to the depression of the thermocline. Figures 5 and 7 give at least some evidence that there was solitary wave activity in the area of acoustic experiments.

Due to the fact that we have no data concerning specific characteristics of internal waves at the experimental site, for simplicity, following Lee's three-layer model of internal wave,²⁹ we assume that the internal wave packet can be expressed by a gated sine function as shown in Fig. 8(b). In this figure, if a packet begins at r_0 , then, for $r_0 + L_p > r > r_0$,

$$Z_1 = 14.0 - 2.0 \sin(2\pi r/\lambda_p), \quad (1)$$

$$Z_2 = 19.0 - 5.0 \sin(2\pi r/\lambda_p). \quad (2)$$

The idealized sound-speed profile in the absence of internal waves for the numerical simulation is shown in Fig. 8(a). We call λ , the soliton wavelength, and L_p , the packet

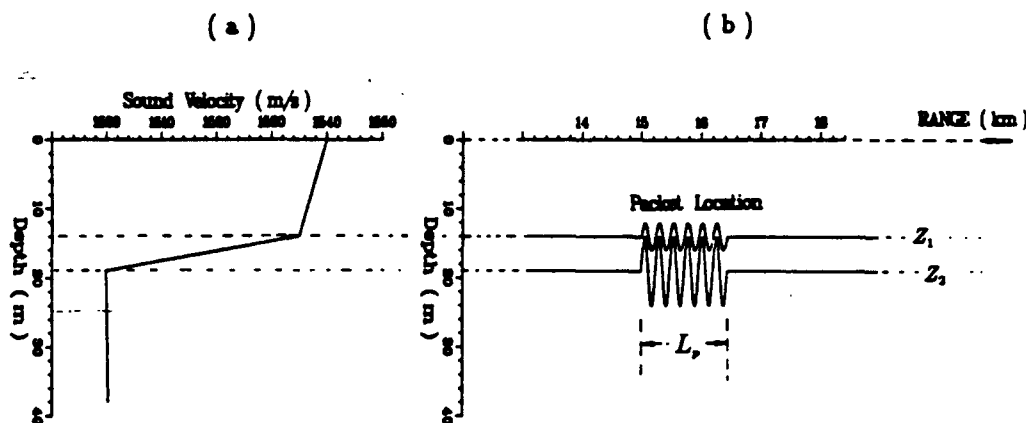


FIG. 8. Simplified oceanic model for an internal wave packet.

length. Referring back to Fig. 1, we see that an almost sinusoidal interface exists between the warmer surface layer and the underlying cooler water. The waveform of the soliton in Fig. 5 of Ref. 1 is also almost sinusoidal. The simplified, sinusoidal model, is thus seen to be not physically unreasonable. The main purpose of this work is to provide the first physical insight into the possible effects of internal wave packets on wideband low-frequency sound propagation in shallow water. It is not to predict the characteristics of internal waves for a specific area. Our simplification should not alter the qualitative results which follow.

The averaged values for bottom sound speed (c_b) and bottom acoustic attenuation (α_p) for the experimental area are given by^{26,30}

$$c_b/c_w = 1.056, \quad (3)$$

$$\alpha_p = 0.34f^{1.44} \text{ dB/m}, \quad (4)$$

where f is the frequency in kHz.

B. Comparison of numerical frequency response with experimental data

Numerical simulation results obtained using the parabolic equation (PE) method (IFD³¹⁻³³ code), show that internal wave packets can significantly change low-frequency transmission loss. The frequency response and, in particular, the abnormal attenuation frequency range are sensitive functions of the parameters of the soliton wave packets.

For example, using the simplified ocean model given in Fig. 8 and Eqs. (1)–(4), we put three internal wave packets located at 5, 15, and 25 km, along propagation track with each packet consisting of six solitons each with a wavelength λ , of 235 m ($L_p = 6\lambda = 1410$ m). The transmission loss as a function of range for four frequencies (with a receiver depth of 32 m and a source depth of 25 m) is shown in Fig. 9. The difference between the results with and without the soliton packets present is small at 100 or 1000 Hz, but at 600 Hz the difference at 30 km is as much as 25 dB. The most interesting and encouraging result is that, in this case the numerical transmission loss as a function of frequency (shown in Fig. 4 by the circles) fits the experimental results quite well.

As a consequence of the characteristics of internal wave packets described in Sec. I (propagation in groups, well-defined wavelengths, high correlation with tides, shoreward propagation), the projection of the solitons in different acoustic propagation directions and for different times will be different. If we change the soliton wavelength in the three packets to 235, 300, 350, 400, and 500 m, we would get frequency responses as shown in Fig. 10, that are similar to the experimental results for different propagation directions shown in Fig. 6. Hence, interaction between acoustic waves and internal wave packets is consistent with Zhou's experimental results for shallow-water sound propagation in the summer.

Why does the abnormally large attenuation in Fig. 4 occur around 630 Hz for internal wave packets consisting of six solitons with a wavelength of 235 m? Why do internal wave packets with the same parameters have a much smaller effect on sound propagation at frequencies around 300 or 1000 Hz? In the next section, we will show that these are due to "resonances" in the acoustic mode-coupling induced by the internal wave packets.

IV. RESONANCE EFFECTS

A. Frequency resonance

For our numerical model of shallow water, with a water depth of 38 m, mode stripping caused by seabottom attenuation, results in only a few modes still being present at a distance of 15 km. If the source and receiver are located below the thermocline, for a realistic sea bottom, the first mode dominates the sound field at long-range over the frequency range of interest. In order to isolate the effect of internal wave packets on the mode coupling among acoustic normal modes, we put a single packet consisting of six solitons with a wavelength of 235 m at 15 km and use the first normal mode alone as the initial input field to the parabolic equation code. Thus, prior to interaction with the packet, we assume only one mode (the first) is present; higher-order modes are generated as the first mode propagates through the internal wave packet. The depth distribution function of

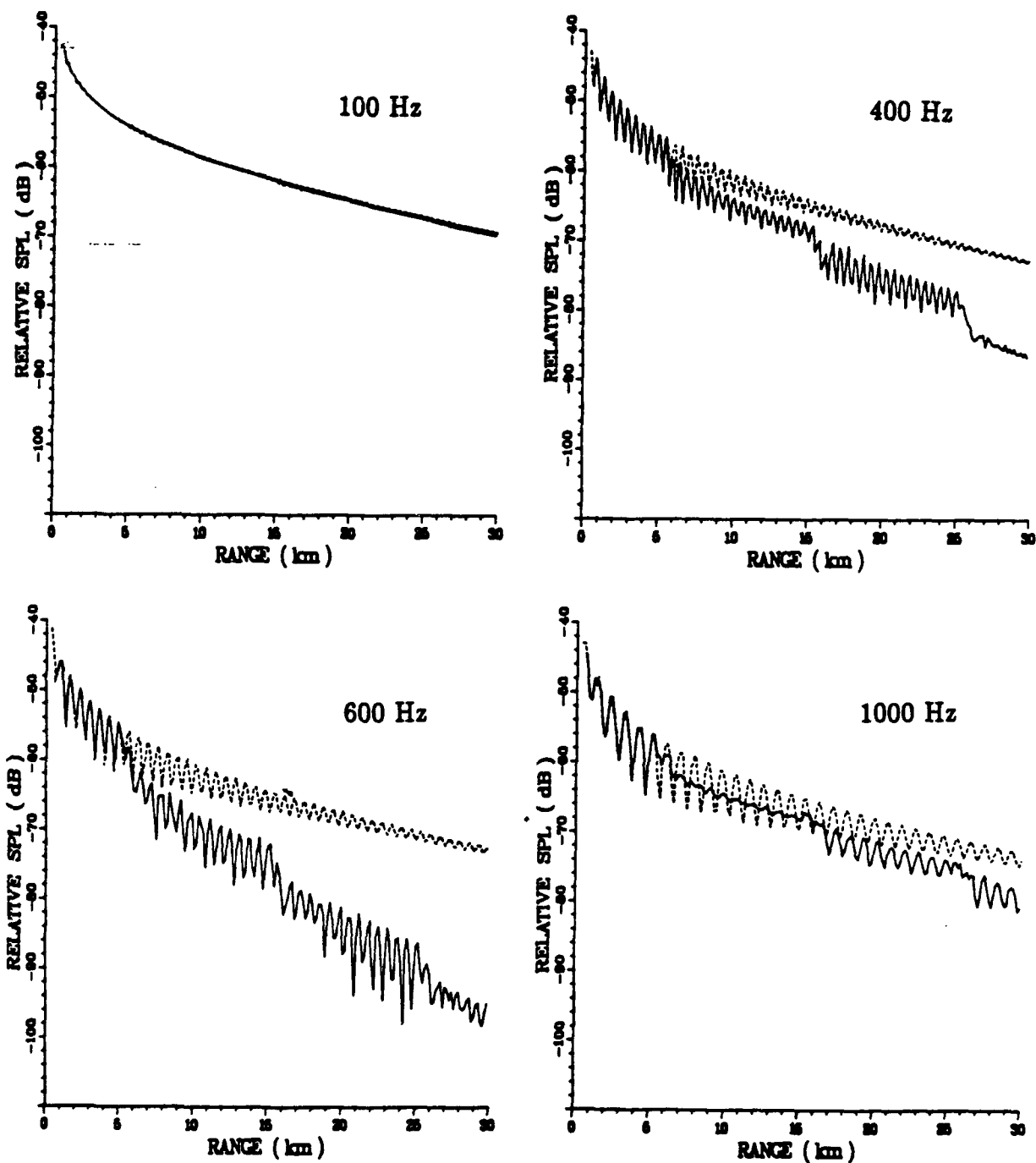


FIG. 9. Comparison between transmission loss without internal waves (---) and with three packets located at 5, 15, and 25 km (—). $L_p = 1410$ m. $\lambda = 235$ m.

sound pressure amplitude at 15, 20, and 30 km obtained by PE method are shown in Fig. 11. At a range of 15 km (before the wave has interacted with the internal wave packet), the shape of the first mode is maintained at all frequencies. After interaction with the internal wave packet, at 300 and 1000 Hz, the energy is still predominantly in the first mode. How-

ever, for 630 Hz, the depth distribution shape is quite different from the first mode, due to resonance scattering, and the amplitude is much smaller.

The mode coupling due to interaction with internal wave packets can be easily calculated. Neglecting the evanescent modes, which decay at large range, leaves only a

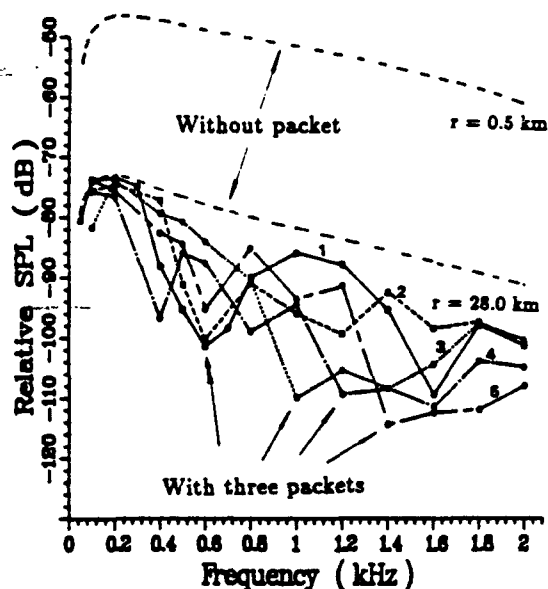


FIG. 10. The computational transmission loss at 28 km for three internal wave packets with different wavelengths λ , = (1) 235 m, (2) 300 m, (3) 350 m, (4) 400 m, (5) 500 m.

finite number of propagating modes at a given frequency. The propagated field $[\Phi_{PE}(r, z)]$ obtained by the PE method can be expanded in terms of a set of local modal eigenfunctions $[U_n(z)]$, corresponding to the sound velocity profile shown in Fig. 8(a), as follows:

$$\Phi_{PE}(r, z) = \sum_n A_{PEn}(r) U_n(z), \quad (5)$$

where the local modal eigenfunctions $U_n(z)$ satisfy the appropriate boundary conditions at the sea surface and bottom and the differential equation

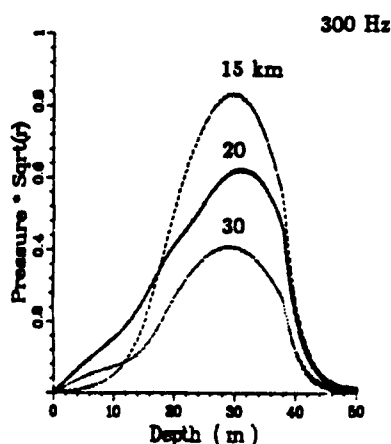
$$\frac{d^2 U_n}{dz^2} + [k^2(z) - k_n^2] U_n = 0, \quad (6)$$

where k_n is the eigenvalue (modal wave number). The modal eigenfunctions also satisfy the orthogonality relation

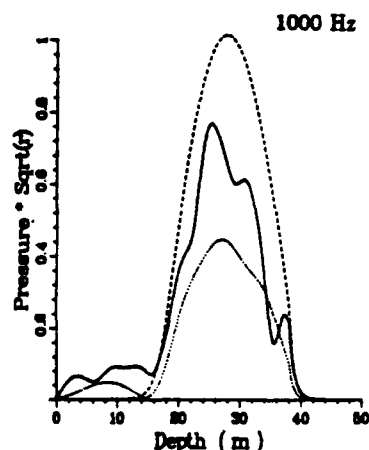
$$\int \rho(z) U_n(z) U_m(z) dz = \delta_{n,m}. \quad (7)$$

The Kronecker delta on the right side is unity if $n = m$ and is zero if $n \neq m$.

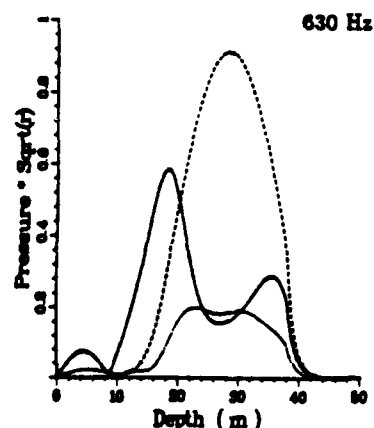
Multiplying both sides of Eq. (5) by $U_m(z)$ and integrating over depth with help of Eq. (7) (mode spatial filtering), we obtain



(a)



(c)



(b)

FIG. 11. The depth distribution function of sound-pressure amplitude for different frequencies at a range of 15 km (---), 20 km (—), and 30 km (—) obtained using the PE method. PE input field: mode 1. One internal wave packet at 15–16.41 km with $\lambda = 235$ m.

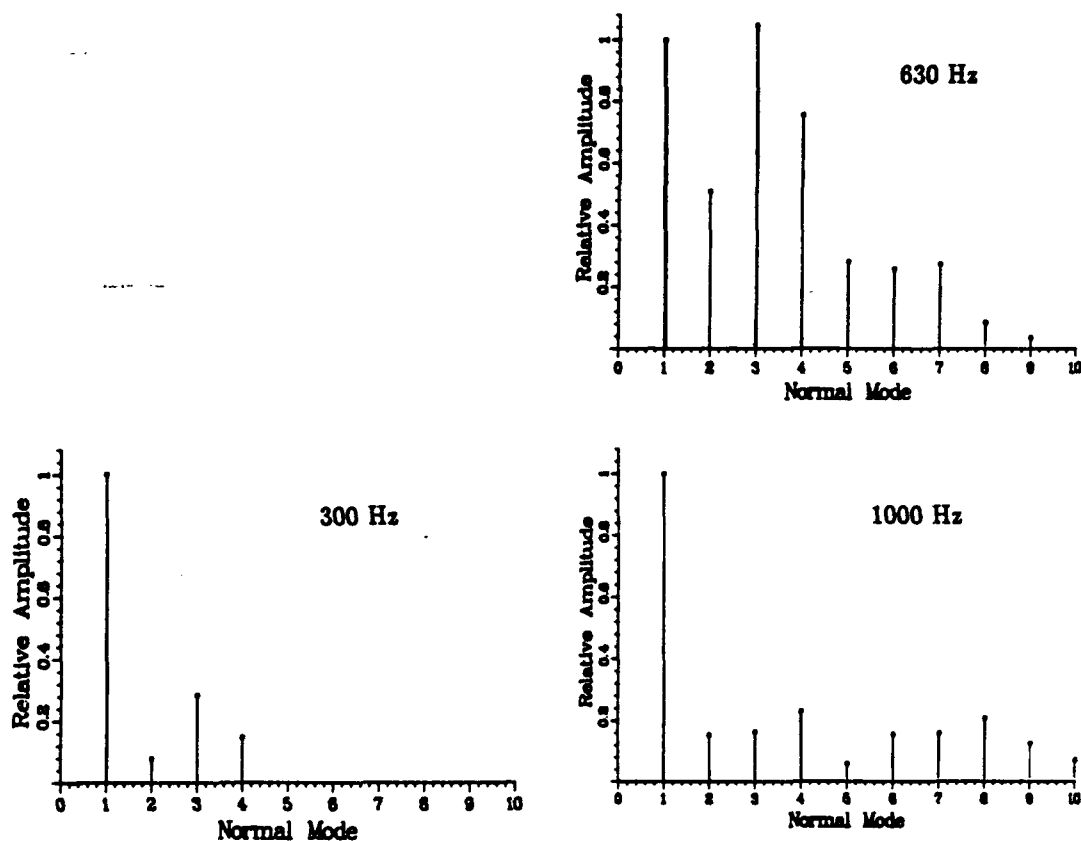


FIG. 12. The relative amplitudes of different modes at 18 km, showing frequency resonance of mode coupling. PE input field: mode 1. One packet at 15–16.41 km. $\lambda_s = 235$ m.

$$A_{PE_n}(r) = \int \rho(z) \Phi_{PE}(r, z) U_n(z) dz. \quad (8)$$

After the interaction of the first mode with the internal wave packet, at selected ranges where no internal wave exists, the relative amplitude of higher-order mode to the first mode, A_{n1} , is given by

$$A_{n1} = \frac{|A_{PE_n}(r)|}{|A_{PE_1}(r)|} = \frac{|\int \rho(z) \Phi_{PE}(r, z) U_n(z) dz|}{|\int \rho(z) \Phi_{PE}(r, z) U_1(z) dz|} = \left(\frac{A_{nR} + A_{nI}}{A_{1R} + A_{1I}} \right)^{1/2}, \quad (9)$$

with

$$A_{nR} = \left(\sum_{j=1}^m \rho_1 \Phi_R(r, z_j) U_n(z_j) + \sum_{j=m+1}^M \rho_2 \Phi_R(r, z_j) U_n(z_j) \right)^2, \quad (10)$$

$$A_{nI} = \left(\sum_{j=1}^m \rho_1 \Phi_I(r, z_j) U_n(z_j) + \sum_{j=m+1}^M \rho_2 \Phi_I(r, z_j) U_n(z_j) \right)^2, \quad (11)$$

where $\Phi_R(r, z_j)$ and $\Phi_I(r, z_j)$ are the real part and the imaginary part of PE field in the j th depth increment, M is the number of layers and the water-bottom interface occurs between the layer m and layer $(m+1)$.³¹ The quantity, A_{n1} , is a measure of the energy exchanged between the first mode and higher-order modes. In this manner using a normal-mode computer program, a PE computer program and the ocean model described in Sec. III, we were able to decompose the sound field obtained from PE into normal modes. The input field for the PE code is the first normal mode. In the absence of modal coupling only this mode would ever be present. Results for three different frequencies are shown in Fig. 12. The plots show the relative modal amplitudes at 18 km. For ranges less than 15 km, only the first mode is present. As indicated in Fig. 12, beyond 15 km there is interaction with the internal wave packet, and at 630 Hz a significant amount of energy has been transferred from mode 1 into higher-order modes that will attenuate rapidly thereafter. Relatively little modal coupling occurs at the other two frequencies. Table I shows the eigenvalue k_n and the attenuation rate β_n (corrected for cylindrical spreading) for the first seven normal modes, calculated by a normal mode program for the sound velocity profile shown in Fig. 8(a) and a frequency of 630 Hz.

TABLE I. The eigenvalue k_n , attenuation rate β_n , and eigenvalue difference between modes 1 and n for the first seven normal modes, $f = 630$ Hz.

Mode n	k_n	β_n (dB/km)	$k_1 - k_n$
1	2.635 594 3	0.2454	0
2	2.626 325 6	0.9169	0.009 268 7
3	2.611 159 6	1.7661	0.024 434 7
4	2.591 298 6	2.4771	0.044 295 7
5	2.572 735 4	1.5938	0.062 858 9
6	2.563 417 2	1.7855	0.072 177 1
7	2.548 399 6	2.3948	0.087 194 7

From this analysis, it is evident that the modal coupling caused by internal waves can sometimes be an important loss mechanism for sound transmission in shallow water in the summer. At 300 and 1000 Hz, the mode-coupling effect is much weaker. Only a few percent of the wave energy is coupled into high-order modes. At 630 Hz, however, a signifi-

cant amount of energy has been transferred from mode 1 into higher-order modes, especially mode 3 and mode 4, with much larger attenuation rate. The mode-coupling induced by internal wave packets exhibits a *frequency resonance* effect, and can cause abnormally large transmission loss around the resonance frequency. The abnormally high attenuation observed by Zhou *et al.* over certain frequency ranges is consistent with interaction with internal waves. In Sec. V, we will discuss what determines the "resonance frequency."

B. Soliton wavelength resonance

We continue to consider a single packet located at a distance of 15 km. We now fix the acoustic frequency at 630 Hz and the packet length (L_p) at 1.4–1.5 km and calculate the effect of soliton wavelength (λ_s) on transmission loss. Figure 13(a) shows the transmission loss as a function of soliton wavelength at a range of 30 km (with a receiver depth

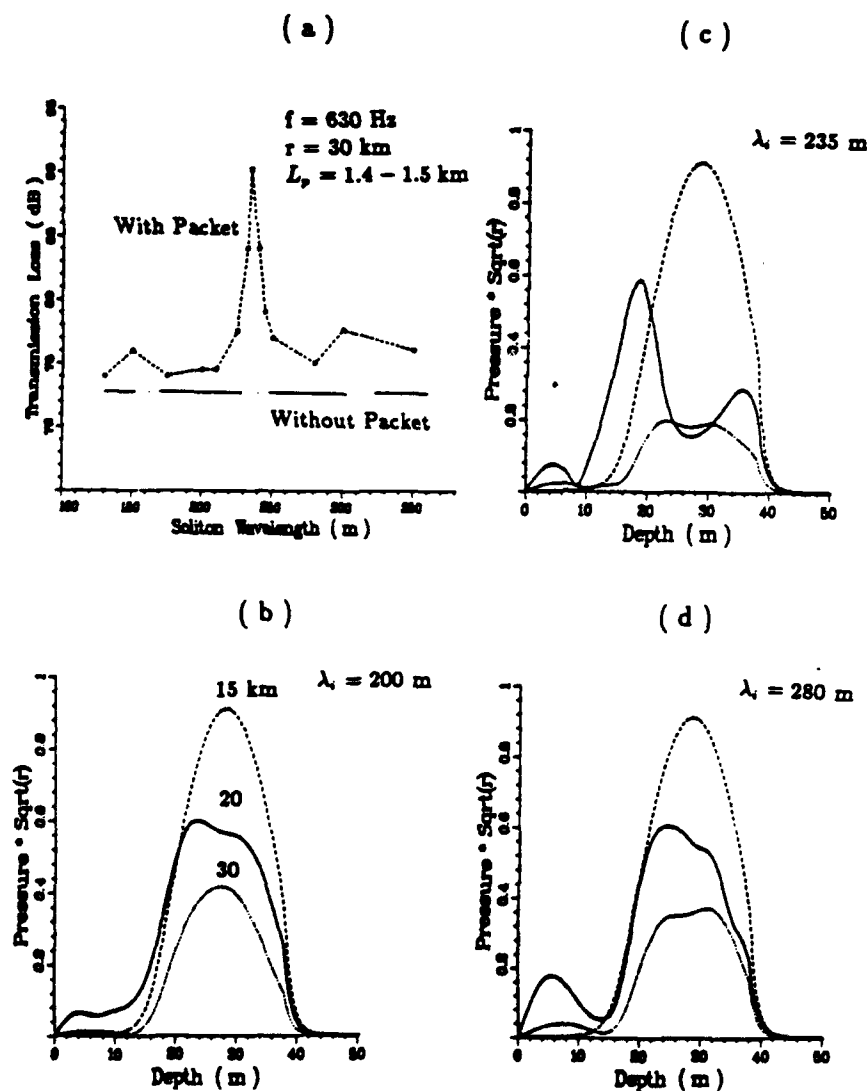


FIG. 13. (a) Soliton wavelength resonance. (b)–(d) The depth distribution function of sound-pressure amplitude for different soliton wavelengths at 15 km (---), 20 km (—), and 30 km (— · —) obtained by PE method. PE input field: mode 1. One packet at 15–16.41 km. $f = 630$ Hz.

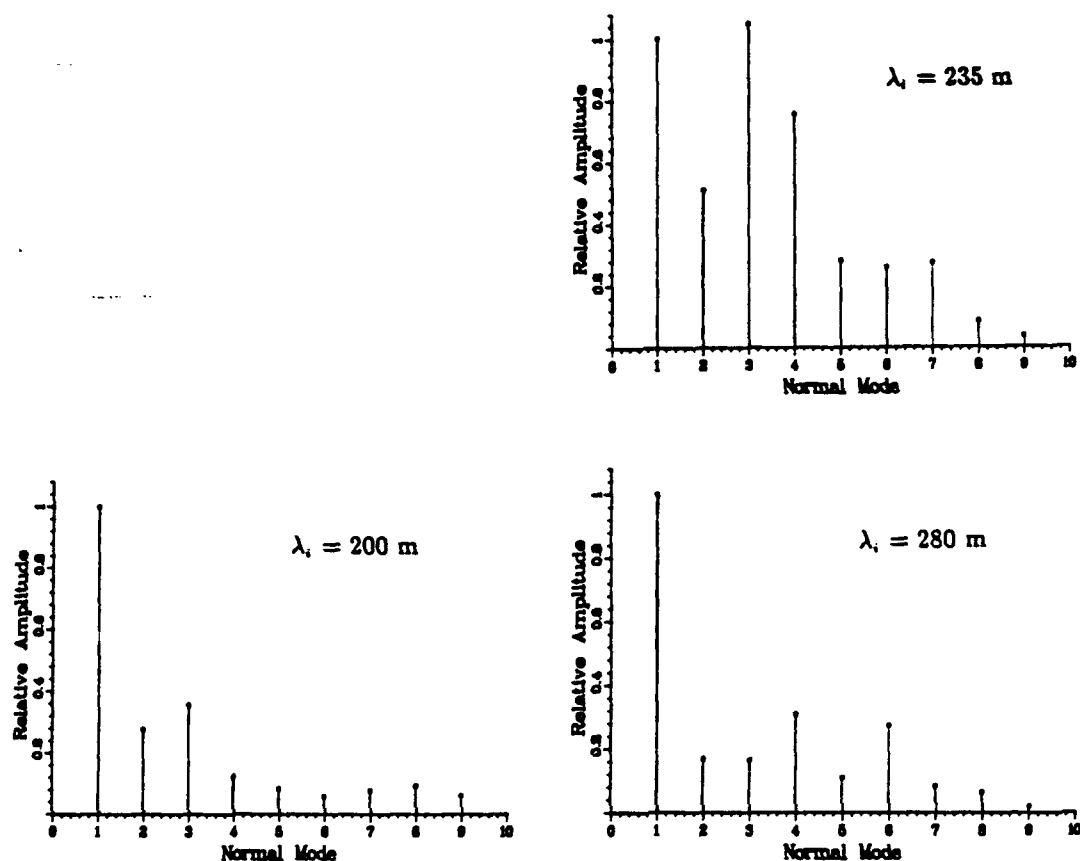


FIG. 14. The relative amplitudes of different modes at 18 km, showing soliton wavelength resonance of mode coupling. PE input field: mode 1. One packet at 15–16.41 km. $f = 630$ Hz.

of 32 m and a source depth of 25 m). Transmission loss exhibits a resonancelike maximum at a soliton wavelength of 235 m. For other soliton wavelengths between 120 and 350 m, the difference between transmission loss with and without the presence of an internal wave packet is not significant. Taking first normal mode as the input field to the PE code, we obtained the depth distribution functions shown in Fig. 13(b)–(d). After interaction with the packet, for a soliton wavelength of 235 m, the shape is very different than that of the first mode, but for 200 and 280 m, the shapes are very close to that of mode 1.

At a distance of 18 km, we again decompose the PE calculated sound field into normal modes and get the results for three different soliton wavelengths shown in Fig. 14. For a soliton wavelength of 235 m, a significant amount of energy has been transferred from mode 1 into higher-order, higher-loss modes. However, for soliton wavelengths of 200 and 280 m, the mode-coupling effect is rather weak. That is, the mode coupling and, hence, the loss induced by internal wave packets exhibits a *soliton wavelength resonance* effect.

C. Packet length resonance

Once again, considering a single packet located at a range of 15 km, we now hold acoustic frequency (630 Hz)

and soliton wavelength (235 m) constant, and calculate the effect of internal wave packet length (or, equivalently, the number of solitons) on transmission loss. Figure 15(a) shows the transmission loss as a function of packet length at 30 km (with a receiver depth of 32 m and a source depth of 25 m). The transmission loss is a periodic, “resonancelike” function of the packet length (L_p). Taking first normal mode as the input field to the PE code, we obtain the depth distribution functions for the sound field for three packet lengths shown in Fig. 15(b)–(d). At 18 km, after interaction with the packet, the shape of the depth distribution function for a six-soliton packet is very different from that of the first mode. However, for a longer packet consisting of 11 solitons it is close to the shape of the first mode and close even in amplitude to the results without a packet.

At a distance of 18 km, we again decompose the PE sound field into normal modes, and get the results for two different packet lengths shown in Fig. 16. For a 1410-m packet (six 235-m solitons), a significant amount of energy has been transferred from mode 1 into higher-order modes. For a longer packet (2585 m, i.e., for 11 solitons), the mode-coupling effect is much weaker. That is, the mode-coupling and hence the loss induced by internal wave packets exhibits a *packet length resonance* effect.

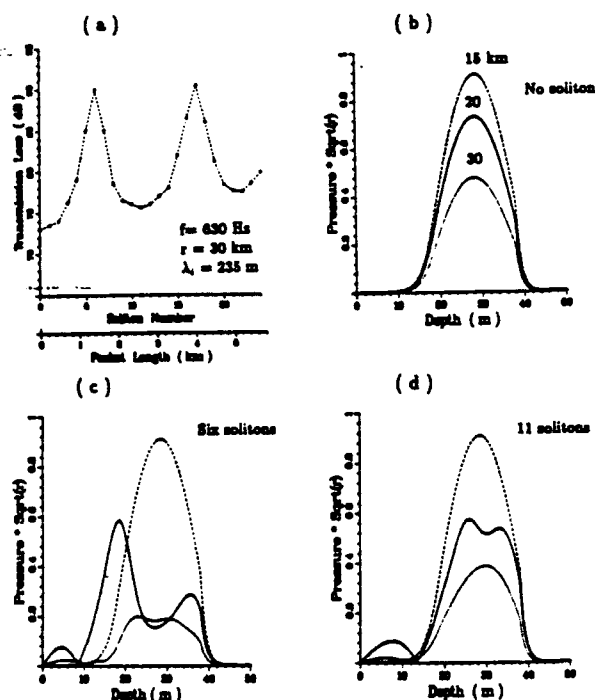


FIG. 15. (a) Packet length resonance. (b)–(d) The depth distribution function of sound-pressure amplitude for different packet lengths at 15 km (---), 20 km (—), and 30 km (---) obtained by PE method. PE input field: mode 1. One packet beginning from 15 km. $f = 630$ Hz.

V. MODAL COUPLING ANALYSIS

Dozier and Tappert,³⁴ and McDaniel and McCammon³⁵ have shown that the exchange of energy between acoustic modes n and m induced by random internal waves in the deep sea or lateral seabed inhomogeneities in shallow water exhibits a wave number resonance effect. The principal transfer of energy will occur between modes whose eigenvalue difference equals the wave number of the spectrum peak of the internal waves or sub-bottom roughness. This result is also applicable to our numerical results shown in Figures 11–14. Significant energy transfer will occur between modes m and n if

$$k_{int} \approx k_n - k_m, \quad (12)$$

where $k_{int} = 2\pi/\lambda_i$ is the wave number of the internal wave. [If the mode coupling is considered to be a quantum mechanical phonon-soliton interaction, Eq. (12) is a statement of conservation of momentum. The corresponding statement of conservation of energy $\omega_{int} = \omega_n - \omega_m$ can be shown to correspond, macroscopically, to the Doppler shift which results from scattering from the moving internal wave.] For our numerical model of internal wave packets with a wavelength of 235 m, the wavenumber of the spectrum peak of the internal wave $k_{int} \approx 2\pi/235 = 0.0267370$. Comparing this value of k_{int} with the eigenvalue differences between mode 1 and mode n shown in Table I, it is found that k_{int} is almost equal to the eigenvalue difference between acoustic normal

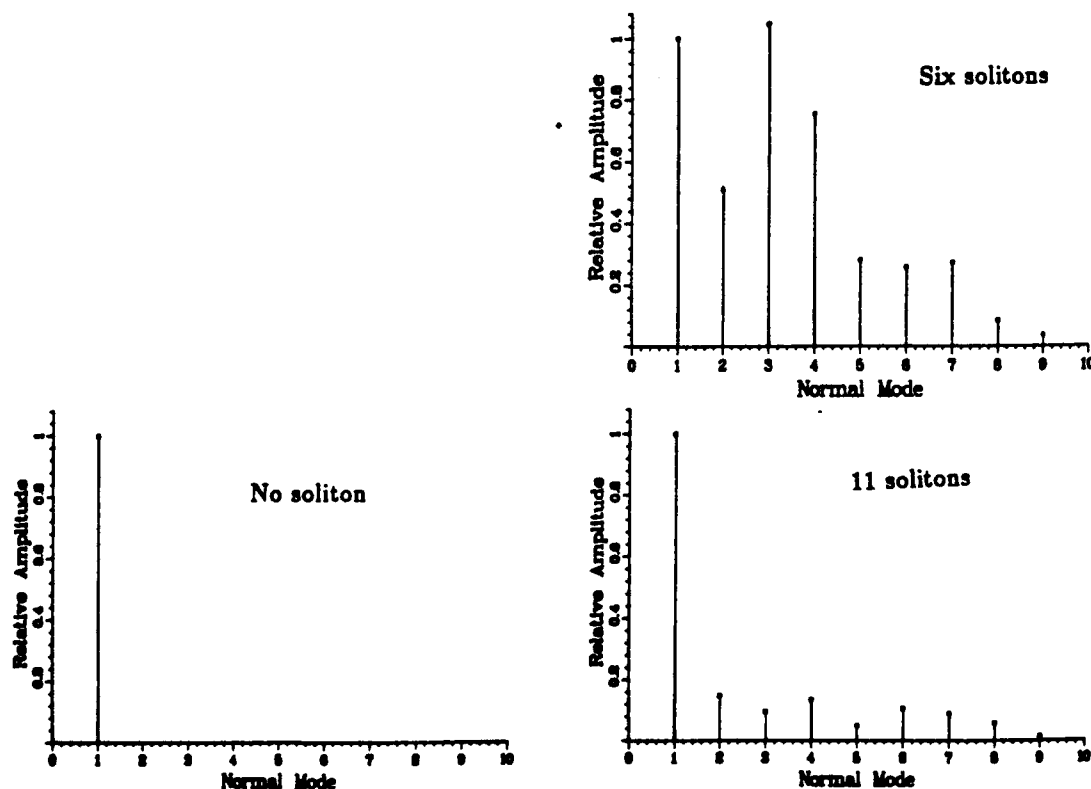


FIG. 16. The relative amplitudes of different modes at 18 km, showing packet length resonance of mode coupling. PE input field: mode 1. One packet beginning from 15 km. $f = 630$ Hz. $\lambda_i = 235$ m.

1 and 3. Thus one would expect a significant amount of energy to be transferred from mode 1 to mode 3 (but not, mode 2). Moreover, k_{1m} is also reasonably close to the differences between the eigenvalues of modes 3 and 4 and modes 4 and 6, etc. Hence, one would expect some transfer of energy from mode 1 to mode 4 via mode 3, or from mode 1 to mode 6 via modes 3 and 4, and so on. These arguments explain why a significant amount of energy is transferred from mode 1 into higher-order modes, especially modes 3 and 4, and why and where the acoustic wave packet and soliton wavelength resonances occur.

The packet length resonance effect mentioned in Sec. IV is so easily explained, and it is still not clear how to predict where it will occur. We present here a preliminary explanation for the phenomenon given by S. T. McDaniel.³⁶ If the backscattered field is neglected, the equation governing mode coupling between m th and n th modes due to range dependence of the ocean environment, can be expressed as Eq. (14) in Ref. 37 for notation]

$$\frac{du_n}{dr} = \frac{1}{2} \sum M_{nm} u_m \exp[i(\bar{k}_m - \bar{k}_n)r]. \quad (13)$$

Let a resonant coupling condition be

$$M_{nm} = -2K_L \exp[-i(\bar{k}_m - \bar{k}_n)r] \quad (14)$$

Let $M_{nm} = -M_{mn}$. We consider only two modes, modes 1 and m , which are assumed to satisfy the resonant coupling condition. From Eqs. (13) and (14), we obtain

$$\frac{du_1}{dr} = -K_L u_m, \quad (15)$$

$$\frac{du_m}{dr} = K_L u_1, \quad (16)$$

$$\frac{d^2 u_{1,m}}{dr^2} + K_L^2 u_{1,m} = 0. \quad (17)$$

If all of the energy is assumed to be initially in the first mode ($u_1 = 1$ and $u_m = 0$) the solution to Eq. (17) is

$$u_1 = \cos(K_L r), \quad (18)$$

$$u_m = \sin(K_L r). \quad (19)$$

Equation (19) predicts that the magnitude of the excitation of higher-order modes will be periodic with range. The resonant coupling parameter K_L determines for what packet lengths u_m has a maximum value (or u_1 has a minimum value). From Eq. (19), the packet length "resonance" will occur when $K_L L_p = (n + 1/2)\pi$. From the first packet length resonance in Fig. 15(a), we have $K_L L_p = K_L \times 235 \times 6 = \pi/2$ and $K_L = 1.11/\text{km}$; from the second resonance length, we have $K_L L_p = K_L \times 235 \times 17 = 3\pi/2$ and $K_L = 1.18/\text{km}$. The two values obtained for K_L are almost the same. The agreement is quite satisfactory considering that the mode coupling occurred between more than just two modes (modes 1 and 3) and K_L would be changed with coupling strength. The mode coupling is a periodic (resonance) function of the internal wave packet length, and hence, acoustic transmission loss at long-range must vary with the packet length. It is shown that the "resonancelike"

behavior of transmission loss predicted by the PE analysis in this paper is consistent with mode coupling theory.

VI. CONCLUSION

In summary, (1) we have briefly reviewed the characteristics of naturally occurring internal wave packets in the coastal zone which differ in many respects from open sea internal waves. We demonstrate that such internal wave packets can have a strong influence on low-frequency long-range sound propagation in shallow water. (2) The measured frequency response of sound propagation during the summer is often a strong function of both time and propagation direction, sometimes the sound propagation has an abnormally large attenuation over some frequency range. (3) Numerical calculations have shown that the interaction between the acoustic waves and internal wave packets and particularly resonance effects in the acoustic mode-coupling induced by internal wave packets could be an important loss mechanism for shallow-water sound propagation in the summer. Modal coupling induced by internal waves could explain the anomalous acoustic experimental results. (4) The fact that the acoustic mode-coupling induced by internal wave packets exhibits *frequency, soliton wavelength, and packet length resonances* [and perhaps existence of the Doppler shift alluded to in Sec. V, as well] suggest that low-frequency acoustic measurements could be used for remote monitoring of internal wave activity and extracting of hydrological and meteorological characteristics of the water mass in the coastal zone.

The analysis and numerical calculations presented here are based on a simplified oceanic model. Although the simplification should not alter the qualitative results presented, a more refined model would be desirable for a more detailed comparison with observations. It is, of course, also possible that some seabottom structure (for example, a surficial layer of low speed), mode-coupling due to the seabed roughness or sediment inhomogeneities and fish shoals could also produce an extra acoustic attenuation over some frequency range. It would thus be desirable for the acoustic, marine geology and geophysics communities including remote-sensing groups to work together to conduct joint at-sea experiments at a specific sea area. If data on internal wave activity (solitary or random), seabottom parameters, and sound propagation were obtained simultaneously and systematically, our understanding of the interaction between internal waves and sound waves in the coastal zone and low frequency acoustic propagation loss in shallow water would be greatly enhanced.

ACKNOWLEDGMENTS

This research was supported by ONR (Grant No. 00014-89-J-1839) and the IAAS. The authors wish to thank Dr. M. H. Orr for his support and valuable suggestions during the course of this research and Dr. S. T. McDaniel for her help in explaining the packet length resonance. The at-sea experiment and data analysis on sound propagation were conducted under the support of the Chinese Academy of

Sciences, while Zhou and Zhang were at the IAAS. J. X. Zhou and X. Z. Zhang would like to express their appreciation to Professor D. Z. Wang and Professor D. H. Guan for their support and helpful comments, to their colleagues at the Institute of Acoustics, especially to E. S. Luo, B. C. Li and Y. Zhang for at-sea experimental assistance and for sharing experimental data.

- ¹ L. Baxter and M. H. Orr, "Fluctuations in sound transmission through internal waves associated with the thermocline: A computer model for acoustic transmission through sound velocity fields calculated from thermistor, CDT, XBT, and acoustic backscattering," *J. Acoust. Soc. Am.* **71**, 61-66 (1982).
- ² E. C. Shang, "Some new challenges in shallow water acoustics," in *Proceedings of 12th ICA Associated Symposium on Underwater Acoustics* (Tech. Univ. of Nova Scotia, Halifax, NS, 1986), pp. 149-152.
- ³ D. H. Guan, "Invited lectures: Some recent progress in shallow water acoustics," *Proc. 13th ICA* **5**, 109-117 (1989).
- ⁴ C. Garrett and W. Munk, "Internal waves in the ocean," *Ann. Rev. Fluid Mech.* **11**, 339-369 (1979).
- ⁵ C. Garrett and W. Munk, "Space-time scales of internal waves," *Geophys. Fluid Dyn.* **2**, 225-264 (1972).
- ⁶ D. Halpern, "Observation on short-period internal waves in Massachusetts Bay," *J. Mar. Res.* **29**, 116-132 (1972).
- ⁷ L. R. Haury, M. G. Melbourne, and M. H. Orr, "Tidally generated internal wave packets in Massachusetts Bay," *Nature* **278**, 312-317 (1979).
- ⁸ M. H. Orr, "Remote acoustic sensing of the oceanic fluid and biological processes," Woods Hole Oceanogr. Inst. Tech. Rep. WHOI-80-2 (1980).
- ⁹ A. R. Osborne and T. L. Burch, "Internal solitons in the Andaman Sea," *Science* **208**, 451-460 (1980).
- ¹⁰ J. R. Apel and F. I. Gonzalez, "Nonlinear features of internal waves off Baja California as observed from the SEASAT imaging radar," *J. Geophys. Res.* **88**, 4459-4466 (1983).
- ¹¹ R. P. Trask and M. G. Briscoe, "Detection of Massachusetts Bay internal waves by the synthetic aperture radar (SAR) on SEASAT," *J. Geophys. Res.* **88**, 1789-1799 (1983).
- ¹² T. D. Allan, *Satellite Microwave Remote Sensing* (Horwood, New York, 1983).
- ¹³ L. L. Fu and B. Holt, "Internal waves in the Gulf of California: observation from a spaceborne radar," *J. Geophys. Res.* **89**, 2053-2060 (1984).
- ¹⁴ H. Sandstrom and J. A. Elliott, "Internal tide and solitons on the Scotian Shelf: a nutrient pump at work," *J. Geophys. Res.* **89**, 6415-6426 (1984).
- ¹⁵ A. K. Liu, J. R. Holbrook, and J. R. Apel, "Nonlinear internal wave evolution in the Sulu Sea," *J. Phys. Oceanogr.* **15**, 1613-1624 (1985).
- ¹⁶ J. R. Apel, J. R. Holbrook, A. K. Liu, and J. J. Tsai, "The Sulu Sea internal soliton experiment," *J. Phys. Oceanogr.* **15**, 1625-1651 (1985).
- ¹⁷ R. D. Pingree and G. T. Mardell, "Solitary internal waves in the Celtic Sea," *Prog. Oceanogr.* **14**, 431-441 (1985).
- ¹⁸ I. S. Robinson, *Satellite Oceanography* (Wiley, New York, 1985).
- ¹⁹ P. E. Holloway, "Internal hydraulic jumps and solitons at a shelf break region on the Australian North West Shelf," *J. Geophys. Res.* **92**, 5405-5416 (1987).
- ²⁰ R. F. Gasparovic, J. R. Apel, and E. S. Kaschke, "An overview of the SAR internal wave signature experiments," *J. Geophys. Res.* **93**, 12304-12316 (1988).
- ²¹ A. K. Liu, "Analysis of Nonlinear internal waves in the New York Bight," *J. Geophys. Res.* **93**, 12317-12329 (1988).
- ²² B. L. Gotwols and R. E. Sterner II, "Measurements of surface wave modulations from internal waves during the SAR internal wave signature experiment," *J. Geophys. Res.* **93**, 12330-12338 (1988).
- ²³ D. C. Honhart, *Oceanography from the Space Shuttle* (UCAR and ONR, Washington DC, 1989).
- ²⁴ K. H. Hunkins and M. Fliegel, "Internal Undular Surges in Seneca Lake: A Natural Occurrence of Solitons," *J. Geophys. Res.* **78**, 539-548 (1973).
- ²⁵ D. M. Farmer, "Observations of long nonlinear internal waves in a lake," *J. Phys. Oceanogr.* **8**, 63-73 (1978).
- ²⁶ J. X. Zhou, "Normal mode measurements and remote sensing of sea-bottom sound velocity and attenuation in shallow water," *J. Acoust. Soc. Am.* **78**, 1033-1008 (1985).
- ²⁷ J. X. Zhou, X. Z. Zhang, P. H. Rogers, and J. Jarzynski, "Geoacoustic parameters in a stratified sea bottom from shallow-water acoustic propagation," *J. Acoust. Soc. Am.* **78**, 2068-2074 (1987).
- ²⁸ Y. P. Zhang (private communication, 1983).
- ²⁹ O. S. Lee, "Effect of an internal wave on sound in the ocean," *J. Acoust. Soc. Am.* **33**, 677-681 (1961).
- ³⁰ J. X. Zhou, X. Z. Zhang, and P. H. Rogers, "Effect frequency dependence of sea-bottom attenuation on the optimum frequency for acoustic propagation in shallow water," *J. Acoust. Soc. Am.* **82**, 287-292 (1987).
- ³¹ D. Lee and G. Botseas, "IFD: An implicit finite difference computer model for solving the parabolic equation," Naval Underwater Systems Center, New London, CT (1982), TR No. 6659.
- ³² G. Botseas, D. Lee, and K. E. Gilbert, "IFD: Wide angle capability," Naval Underwater Systems Center, New London, CT (1983), TR No. 6905.
- ³³ D. Lee, "The State-of-the-art Parabolic Equation approximation as applied to underwater acoustic propagation with discussion on intensive computations," an invited paper at 108th ASA meeting, and NUSC Tech. Rep. 7247 (1984).
- ³⁴ L. B. Dozier and F. D. Tappert, "Statistics of normal mode amplitudes in a random ocean. 1. Theory," *J. Acoust. Soc. Am.* **63**, 353-365 (1978).
- ³⁵ S. T. McDaniel and D. F. McCammon, "Mode coupling and the environmental sensitivity of shallow-water propagation loss predictions," *J. Acoust. Soc. Am.* **82**, 217-223 (1987).
- ³⁶ This was pointed to us by Dr. S. T. McDaniel (private communication).
- ³⁷ S. T. McDaniel, "Mode coupling due to interaction with the seabed," *J. Acoust. Soc. Am.* **72**, 916-923 (1982).